Quaternary Science Advances 15 (2024) 100212

Contents lists available at ScienceDirect

Quaternary Science Advances

journal homepage: www.sciencedirect.com/journal/quaternary-science-advances

Last interglacial and MIS 9e relative sea-level highstands in the Central Mediterranean: a reappraisal from coastal cave deposits in the Cilento area, Southern Italy

Ilaria Isola [a,*], Monica Bini [a,b,c], Andrea Columbu [b,c], Mauro Antonio Di Vito [d], Biagio Giaccio [e], Hsun-Ming Hu [f,g], Fabio Martini [h], Francesca Pasquetti [b], Lucia Sarti [i], Federica Mulè [b], Antonio Mazzoleni [j], Chuan-Chou Shen [f,g], Giovanni Zanchetta [a,b,c]

[a] Istituto Nazionale di Geofisica e Vulcanologia (INGV), sez. Pisa, Pisa, Italy
[b] Department of Earth Sciences, University of Pisa, Via S. Maria, 56126, Pisa, Italy
[c] Centre for Climatic Change Impact (CIRSEC), University of Pisa, Pisa, Italy
[d] Istituto Nazionale di Geofisica e Vulcanologia (INGV): Osservatorio Vesuviano, Naples, Italy
[e] Istituto di Geologia Ambientale e Geoingegneria, Consiglio Nazionale delle Ricerche, 00015, Montelibretti, Rome, Italy
[f] High-Precision Mass Spectrometry and Environment Change Laboratory (HISPEC), Department of Geosciences, National Taiwan University, Taipei, 10617, Taiwan
[g] Research Center for Future Earth, National Taiwan University, Taipei, 10617, Taiwan
[h] Dipartimento di Storia, Archeologia, Geografia, Arte e Spettacolo, University of Florence, Prehistory Unit, Via S.Egidio 21, 50122, Firenze, Italy
[i] Dipartimento di Scienze storiche e dei Beni culturali, University of Siena, Via Roma 56, 53100, Siena, Italy
[j] Onorary Inspector for Archaeology of Salerno Province, Ministero per i Beni e Le Attività Culturali, Rome, Italy

ARTICLE INFO

Keywords:
Lithophaga burrows
Notches
Last interglacial highstand
MIS 5e
MIS 9e highstand
U/Th dating
Speleothems
Cilento
Southern Italy

ABSTRACT

A revaluation of the relative sea-level (RSL) indicators in the Baia di Infreschi (Cilento, Southern Italy) supported by new 30 U/Th dating on speleothems indicates that the upper level of *Lithophaga* burrows identified by Bini et al. (2020) at ~9 m a.s.l. and correlated to the Last Interglacial (LIG) highstand should be referred to the highstand of the MIS 9e, whereas the local RSL for the highstand of the LIG is now reassessed at 5.3 ± 0.18 m a.s.l. The upper level of the *Lithophaga* marker can be followed for ~12 km along the coast, suggesting a substantial absence of important relative tectonic movements. In the Baia di Infreschi an additional marine indicator, a notch sealed by a flowstone dated ~110 ka, indicates several phases of RSL stationing below the maximum highstand of the LIG. The presence of flowstones as low as 2 m a.s.l. dated to the MIS 7 shows that the highstand of MIS 7 was probably below the present sea level. All these evidences allow us to reassess the stratigraphy of some archaeological caves in the area, indicating that the sedimentary successions preserved there are older than what was previously believed.

1. Introduction

The Last Interglacial (LIG) marine highstand, roughly corresponding to marine isotope stage 5e (MIS 5e, Govin et al., 2015; Rovere et al., 2016; Dutton et al., 2015), has left several morphological and sedimentological traces worldwide. These have been used for the reconstruction of the past relative sea level (RSL, e.g. van de Plassche, 1986; Shennan et al., 2000; Rovere et al., 2016; Rovere et al., 2023), to constrain geophysical models and fingerprint ice-cap melting and cryosphere response to climate (Dutton and Lambeck, 2012; O'Leary et al., 2013; Dutton et al., 2015; Rohling et al., 2019). Different data sets (in particular those from far-field locations – i.e. sites located far from the glacioisostatic effect of large ice sheets) indicate that the sea level was globally above the present sea level (a.s.l.) with an estimation of up to 9 m (e.g., Kopp et al., 2009; Dutton and Lambeck, 2012; O'Leary et al., 2013; Dutton et al., 2015). Based on U/Th dating on corals this phase of sea-level highstand may have occurred from ~129 to 116 ka (e.g. Stirling et al., 1998; Muhs, 2002; Muhs et al., 2015). However, the general regional trends and the timing, magnitude and dynamics of the RSL during the LIG are subject to an intense debate and can show regional differences (e.g., Stirling et al., 1998; Esat et al., 1999; Hearty et al., 2007; Moseley et al., 2013; Polyak et al., 2018; Rohling et al.,

* Corresponding author.
E-mail address: ilaria.isola@ingv.it (I. Isola).

https://doi.org/10.1016/j.qsa.2024.100212
Received 5 April 2024; Received in revised form 8 June 2024; Accepted 11 June 2024
Available online 19 June 2024

2019). For instance, by comparing LIG sea-level data across the Bahamian archipelago with a suite of Glacial Isostatic Adjustment (GIA) models, Dyer et al. (2021) concluded that there is a 95% probability that the global sea level peaked at least 1.2 m a.s.l., and that it is very unlikely (5% probability) to have exceeded 5.3 m. More recently, for the same area, Dumitru et al. (2021) indicated the MIS 5e between 1 and 2.7 m a.s.l. corrected for GIA and long-term subsidence. On Mallorca Island (Western Mediterranean), phreatic overgrowths on speleothems indicate that the MIS 5e sea level in this region was within a range of 2.15 ± 0.75 m a.s.l. (Polyak et al., 2018).

In the Mediterranean basin, the coastal marine sediments associated with the LIG highstand have been historically termed "Tyrrhenian" deposits (Issel, 1914; see review in Asioli et al., 2005, and references therein), often characterized by the presence of the iconic warm-water mollusc *Thetystrombus latus* (formerly *Strombus bubonius*, then *Persististrombus latus*, e.g. Taviani, 2014). Many of these deposits have been dated using the U/Th method applied to marine fossils (e.g. Hillaire-Marcel et al., 1996; Jedoui et al., 2003; Muhs et al., 2015). However, according to Pasquetti et al. (2021), most of the U/Th ages obtained on marine fossil remains performed in the last decades in the Mediterranean region do not pass strict geochemical criteria for quality and thus should be considered carefully. Indeed, because of the tendency of fossil remains to incorporate/lose U during early diagenesis, the chronology for many Tyrrhenian deposits demands a reappraisal. Dating of phreatic overgrowths on speleothems (POS) offers an interesting novel alternative to traditional U/Th dating on corals and/or on molluscs in order to constrain the age of the LIG highstand (e.g. Polyak et al., 2018; Dumitru et al., 2021, and references therein) as well as any sea level standstill (Lončar et al., 2024). However, POS are relatively rare in coastal caves and their analysis necessitates removal, hence compromising the conservation of this uncommon specimen in its natural heritage (Columbu et al., 2021). Alternative dating methods have been applied to the clastic deposits or to fossil remains (e.g., optical-stimulated luminescence Mauz, 1999; amino-acid racemization, Hearty et al., 1986) but they usually yielded lower chronological accuracy and precision (e.g. Mauz, 1999; Cerrone et al., 2021a). Dating detrital sanidine in areas characterized by intense volcanic explosive activity by the $^{40}Ar/^{39}Ar$ method can further constrain the age of the deposits, but the method only provides information on minimum age, i.e., *terminus post quem* for the marine-coastal sediments (e.g., Marra et al., 2020). An additional approach is to use speleothems (vadose cave calcite deposits, e.g. Bard et al., 2002; Moseley et al., 2013; De Waele et al., 2018; Lucia et al., 2021), which usually represent reliable material for high-precision U/Th dating, despite the inconvenience of providing only the chronology of the terrestrial limiting point. In other words, the RSL was certainly lower than the location of the dated speleothem, but the exact elevation is indefinable (Rovere et al., 2015). Nevertheless, recent studies indicate that an intense and systematic application of speleothem U/Th dating in coastal caves can represent a powerful chronological tool for outlining the timing of the LIG highstand, especially to assess the age of its conclusion (e.g., Bini et al., 2020; Giaccio et al., 2024).

Here we present a new set of stratigraphic evidence supported by novel U/Th ages obtained on cave speleothems from the Baia di Infreschi coastline, in the Cilento area, southern Italy (Fig. 1), where previous investigations allowed to infer on the dynamics of the LIG highstand. Our results made it possible to reappraise the maximum RSL elevation during the LIG highstand, to improve the chronology of its demise and to unveil the presence of a previously undetected, older highstand phase related to MIS 9e.

2. Site description and previous investigations

The studied area is located along the Cilento Promontory, southern Italy (Fig. 1), a large structural high between the gulfs of Salerno and Policastro. The work was mainly conducted in the embayment of Baia di Infreschi (39°59′57″N, 15°25′33″E), which hosts several karst features among which the Infreschi and Coral caves. Furthermore, observations and U/Th dating were also extended to the area between Marina di Camerota and Palinuro Harbour (Fig. 1). This area is dominated by limestone and cherty limestone of the Mt Bulgheria Mesozoic-Cenozoic units (Ascione et al., 1997; Ascione and Romano, 1999). During the Quaternary, the area was affected by extensional tectonics linked to the counterclockwise rotation of the Italian peninsula related to the roll-back of the lithospheric slab (e.g., Facenna et al., 2013). According to Ferranti et al. (2006), who analysed the position of the regional elevation of the LIG highstand sea-level markers, the studied area is considered tectonically almost stable, with vertical movement estimates from ~0.03 to ~0.07 mm/yr for the last ~125 kyr. The area is microtidal with maximum tidal range of ~40 cm (Palinuro Tidal Station; https://www.mareografico.it [accessed 08/05/2024]).

The Infreschi Cave succession (called *Riparo degli Infreschi* – literally Infreschi Shelter in Sarti, 1996; Esposito et al., 2003) represents the remaining infilling of a partially collapsed cavern (Sarti, 1996; Esposito et al., 2003; Martini, 2015). According to the stratigraphy proposed by Bini et al. (2020), it contains seven main lithostratigraphic units (LU)

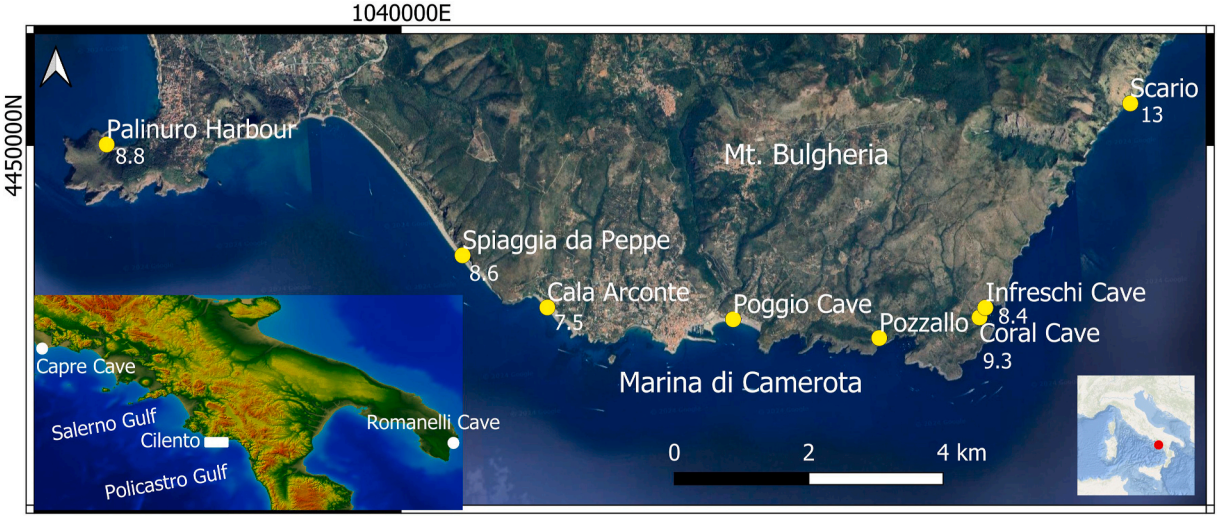

Fig. 1. The study area, with sampling sites marked by yellow circles. The numbers indicate the maximum elevation (m a.s.l.) of Lithophaga burrows. The main localities cited in the text are highlighted. (For interpretation of the references to colour in this figure legend, the reader is referred to the Web version of this article.)

developed on the local carbonate substratum (LU-1 to 7, Fig. 2a). The older unit (LU-1) is composed of a cemented gravelly beach deposit in a sandy matrix with sparse marine fossils tentatively attributed to MIS 9e by Bini et al. (2020). The LU-1 is covered by a first phase of flowstone and stalagmite deposition (LU-2, Fig. 2a), with U/Th ages ranging from ~239 to 199 ka (e.g. MIS 7–8). Both surfaces of LU-1 and LU-2 are densely riddled with *Lithophaga* burrows (Fig. 2a), which terminate in a straight horizontal limit at ~8.7 m (above the local biological marker) on the vertical cave walls. LU-3 represents a second gravel beach deposit with a sandy matrix containing abundant mollusc remains. U/Th dating of these molluscs yielded inconsistent results from ~145 to 77 ka, showing a generic MIS 5 highstand. LU-3 is overlain by well-stratified and well-sorted medium sands of aeolian origin (LU-4, Fig. 2a and b). Both LU-3 and LU-4 cover the *Lithophaga* burrows, indicating that they are younger than the boreholes. This succession is in turn capped by a typical "Terra rossa" paleosol (LU-5) (Esposito et al., 2003). This succession has been partially eroded and dismantled and is covered by a flowstone (LU-6, Fig. 2a), which forms a complex curtain-like succession of wall draperies partially covering the older LUs. LU-6 was dated in the lower levels at different stratigraphic locations from ~120 to 111 ka. The undated higher draping flowstone from LU-6, without Lithophaga burrows but still covering the higher level of burrows on the cave walls, was instead assumed by Bini et al. (2020) to belong to the same generation of the Late MIS 5e speleothems, or younger, in agreement with other previous works on the same site (e.g. Esposito et al., 2003). Finally, according to Bini et al. (2020), the described succession was partially carved and then filled with a continental deposit (LU-7, see Fig. 2a) comprising blocks, breccias with a reddish matrix, and sandy-to-silty deposits, embedding Middle Paleolithic artefacts and bone remains ("Musterian", Sarti, 1996; Martini, 2015). The continental clastic succession contains a decimetric-thick massive tephra layer chemically fingerprinted and correlated to the Maddaloni/X-6 ash layer with an age of ~109 ka (Bini et al., 2020; Zanchetta et al., 2018; Monaco et al., 2022).

Summarizing, based on the above-described set of morpho-stratigraphic and geochronological data, Bini et al. (2020) concluded that: i) the RSL during the LIG highstand locally peaked at 8.90 ± 0.6 m a.s.l.; ii) the sea level dropped rapidly before ~120 ka for at least 6 m, i.e., at an elevation >3 m a.s.l.; iii) there was no evidence of RSL rise after this period above the present sea level; and iv) there were older marine deposits, possibly attributable to MIS 9, represented by a coastal marine conglomerate, but no accurate sea-level markers were found for the related highstand. However, all the upper flowstones and columns (indicated with LU-6 in Fig. 2a) not riddled by *Lithophaga* burrows were not included in the sampling by Bini et al. (2020), thus leaving the correlation of this carbonate deposition to the one dated between ~120 and 111 ka. Therefore, the attribution of the 8.90 ± 0.6 m a.s.l. highstand to the LIG is a reasonable but not a definitively proven hypothesis.

3. Material, methods and sampling strategy

3.1. Field campaigns

New fieldwork was conducted in 2021 and 2022 in the entire Baia di Infreschi and was expanded in the nearby areas of the Cilento promontory (Fig. 1). This work included new stratigraphic observations in the already investigated Infreschi Cave and at the new site of the Coral Cave (named, in Italian, "*La Grotta dei Coralli*" by Martini, 2015, and called Infreschi Cave in Esposito et al., 2003, Fig. 1). New speleothem samples were collected for a set of novel U/Th dating (n = 30).

3.2. Sea-level indicator measurements

We considered different sea-level indicators such as *Lithophaga* burrows, notches, marine caves, speleothem deposition, and wave-cut terraces, where the first two are the most frequent. *Lithophaga lithophaga* is an endolithic bivalve living inside carbonate rocks from the upper limit of the infralittoral zone down to more than 30 m in depth. When present, the upper almost linear limit of burrows is an accurate fixed biological indicator and it coincides closely with the sea level (Laborel and Laborel-Deguen, 1994, 2005; Rovere et al., 2015). This limit has been widely used as a sea-level indicator around the Mediterranean basin (Lambeck et al., 2004; Ferranti et al., 2006; Antonioli and Oliverio, 1996). However, when only isolated groups of burrows are present, without a well-defined straight upper limit, they can only be used as a lower limit. Tidal notches are indentations in rocky coasts shaped by the interplay of different processes such as bioerosion, wave action, tidal wetting and drying cycles together with karst processes on limestone coasts (Antonioli et al., 2015; Carobene, 2015; Pirazzoli et al., 1996). Their inner vertex is considered a very accurate paleo-sea-level indicator, particularly in microtidal environments (Ferranti et al., 2006; Antonioli et al., 2007; Pirazzoli, 2007; Stewart and Morhange, 2009). When possible, the elevations of each indicator were measured using a Trimble R10 GNSS (maximum error in elevation of acquired points was

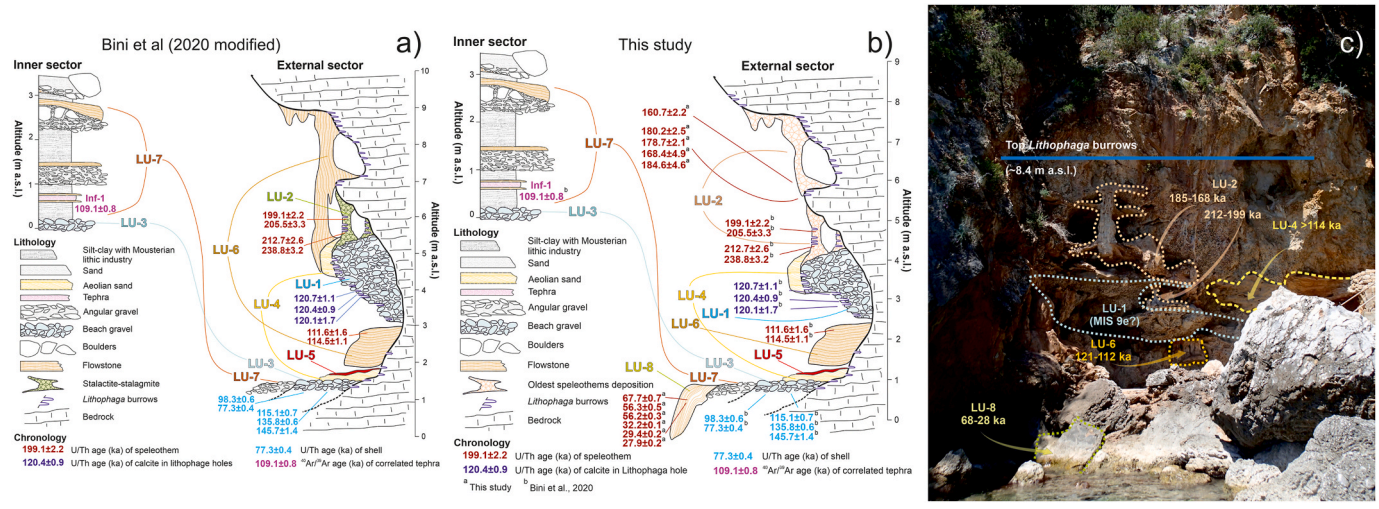

Fig. 2. The Infreschi Cave stratigraphy. a) Lithostratigraphic Units (LU) and geochronology of the Infreschi Cave (after Bini et al., 2020, modified). b) Lithostratigraphic Units (LU) and geochronology of the Infreschi Cave in this study. The units from LU-1 to LU-7 have already been described by Bini et al. (2020), LU-8 has been described here for the first time. The elevation axis is not in scale. It is only used to allow a comprehensive view of all the units. c) General view of the western sector of the Infreschi Cave highlighting the main morpho-stratigraphical features.

0.14 m). The data were acquired by the WGS84 Geographic Coordinate System and post-processed and referred to the geoid model ITALGEO2005 (millimetric planimetric error and ±0.035 m elevation error). Where the direct measurement with R10 was not possible (e.g. inside the caves or close to the marine cliff), we used a graduated rod equipped with a spirit level (repeated measurements of our research group on the same sea-level indicators with this method yielded associated errors that were usually within ±0.1 m; Zanchetta et al., 2014; Bini et al., 2014; Bini et al., 2018, 2020; Giaccio et al., 2024). In some circumstances, the elevations were measured directly referring to the local biological mean sea level (i.e. organisms anchored to hard substrates and their living upper range, located near or at sea level, Rovere et al., 2015). The biological mean sea level in microtidal Mediterranean settings corresponds to the mean sea level with reasonable accuracy (±0.1 m, e.g., Vacchi et al., 2020, and reference therein). Where logistically possible, the local biological mean sea level was measured with R10 to facilitate comparison with previous works in the same area (e.g. Bini et al., 2020; Esposito et al., 2003).

The measurements indicate that the local biological mean sea level at Baia di Infreschi is located 0.35 ± 0.39 m below the geodetic sea level (hereafter, the measurements will be referred to as the local geoid). The final altitude error of each marker is calculated following e.g. Shennan et al. (2000), and it includes the different errors in the measure of altitude (vertical precision of the finest R10 measure, post-processing error, the error associated with the use of spirit bars).

3.3. Sampling strategy

To constrain the position of the second generation of the Infreschi Cave *Lithophaga* burrows we defined the limit between the flowstone LU-2 riddled with burrows and the flowstone without burrows of the same generation. The riddled sample was dated by Bini et al. (2020). We then sampled the lowest level of the flowstone not riddled by *Lithophaga* to obtain an upper level to constrain the LIG highstand (samples INF20–7I, INF20-7E; Table 1, Fig. 3). We also collected an additional flowstone outcropping in the lower section of the cave and covering red continental breccias (LU-7 of Bini et al., 2020). This new unit, which dips ~30 cm below the present-day sea level, was labelled as LU-8 (Fig. 2b and c, Sample INF20-1, INF20-2; Fig. 3, Table 1). On the southern side of the Infreschi Cave, the flowstone covering the cave wall with *Lithophaga* burrows was also sampled (INF-13; Fig. 3, Table 1). Additional speleothems associated with different marine erosive features were sampled in all the Baia di Infreschi (Fig. 3). Four different flowstones were collected close to the Coral Cave (BIO-7, BIO-8, INF20-3, INF-20-4; Table 1, Fig. 3). They were relatively eroded and two of them covered a cemented marine conglomerate (Fig. 3). An additional flowstone covering two different sets of notches in the Baia di Infreschi was collected not far from Coral Cave (INF20-5; Fig. 3). Along the nearby Marina di Camerota coast, two additional flowstones were sampled at Cala di Arconte and at the Pozzallo beaches. The former, situated at approximately 2 m a.s.l., is a highly eroded flowstone covering a continental deposit and a rocky surface with *Lithophaga* burrows (Sample STC22-1, STC22-2; Table 1, Fig. 3). The latter covers a cemented marine conglomerate at approximately 1.5 m a.s.l. (Sample POZZ22-1; Table 1, Fig. 3).

3.4. Sample preparation and U/Th dating

Calcite chips were removed from the freshly cut and polished speleothem surfaces by using a hand microdrill, and were aimed at U/Th

Table 1
Uranium and thorium isotopic compositions and 230Th ages by MC-ICPMS, Thermo Electron Neptune, at NTU.

Site	LU	Sample ID		^{238}U 10^{-9}g/g [a]		^{232}Th 10^{-9}g/g		$\delta^{234}U$ measured[a]		$[^{230}Th/^{238}U]$ activity[c]		$^{230}Th/^{232}Th$ atomic ($\times 10^{-6}$)		Age (kyr ago) uncorrected		Age (ka) corrected [c,d]		$\delta^{234}U_{initial}$ corrected[b]		Elevation on marker (m)	Elevation a.s.l. (m)	Marker elevation on geoid (m)
Infreschi Cave	8	INF20-1	Top1	3280.5	± 3.9	11.558	± 0.036	38.4	± 1.4	0.4200	± 0.0015	1965.7	± 9.2	56.32	± 0.29	56.16	± 0.29	44.9	± 1.6	0.7	0.35	-0.35
			Top2	654.46	± 0.86	6.125	± 0.021	33.2	± 3.3	0.4197	± 0.0024	739.3	± 4.8	56.65	± 0.49	56.33	± 0.50	39.0	± 3.9	0.7	0.35	-0.35
			Base2	1268.1	± 1.6	19.66	± 0.10	36.4	± 2.4	0.4833	± 0.0031	513.9	± 4.2	68.16	± 0.66	67.69	± 0.68	44.1	± 2.9	0.7	0.35	-0.35
		INF20-2	1	1344.2	± 1.4	7.490	± 0.021	34.6	± 1.4	0.2358	± 0.0010	697.7	± 3.4	28.16	± 0.14	27.95	± 0.16	37.5	± 1.5	0.6	0.25	-0.35
			2	1584.4	± 1.6	15.281	± 0.058	39.3	± 1.4	0.2485	± 0.0013	424.9	± 2.7	29.75	± 0.18	29.43	± 0.22	42.7	± 1.5	0.6	0.25	-0.35
			3	964.06	± 0.95	2.386	± 0.008	34.4	± 1.3	0.26564	± 0.00071	1770.0	± 7.6	32.31	± 0.11	32.17	± 0.12	37.7	± 1.4	0.6	0.25	-0.35
	2	INF-10		116.31	± 0.13	1.786	± 0.010	27.2	± 2.0	0.7972	± 0.0044	856.1	± 6.6	161.19	± 2.19	160.73	± 2.19	42.9	± 3.2	6.5	6.15	-0.35
	2	INF-13		232.06	± 0.25	55.28	± 0.34	37.8	± 1.5	0.8913	± 0.0030	61.69	± 0.43	207.80	± 2.32	201.66	± 3.82	66.8	± 2.8	4.2	3.85	-0.35
	2	INF21-7I	1	273.53	± 0.26	7.891	± 0.026	23.9	± 1.3	0.8333	± 0.0043	476.3	± 2.9	180.96	± 2.46	180.15	± 2.47	39.7	± 2.1	6.0	5.65	-0.35
			2	286.72	± 0.29	5.360	± 0.016	23.7	± 1.3	0.8300	± 0.0037	732.0	± 3.8	179.23	± 2.13	178.68	± 2.13	39.3	± 2.2	6.0	5.65	-0.35
	2	INF21-7E	1	179.96	± 0.18	32.03	± 0.16	28.2	± 1.5	0.8226	± 0.0087	76.21	± 0.89	173.08	± 4.47	168.41	± 4.89	45.3	± 2.5	6.0	5.65	-0.35
			2	155.13	± 0.14	15.272	± 0.068	26.4	± 1.5	0.8468	± 0.0076	141.8	± 1.4	187.16	± 4.48	184.57	± 4.56	44.4	± 2.5	6.0	5.65	-0.35
Baia Infreschi		INF20-3	1	480.63	± 0.59	6.050	± 0.017	15.9	± 3.2	0.8739	± 0.0032	1144.6	± 5.1	212.00	± 3.51	211.6	± 3.50	28.9	± 5.9	2.2	1.98	-0.22
			2	542.49	± 0.50	39.49	± 0.22	13.6	± 1.3	0.8752	± 0.0070	198.2	± 1.9	214.87	± 5.49	212.91	± 5.48	24.7	± 2.5	2.2	1.98	-0.22
			3	562.88	± 0.61	56.861	± 0.38	12.5	± 1.3	0.8792	± 0.0088	143.5	± 1.7	218.82	± 7.09	216.10	± 7.05	23.1	± 2.5	2.2	1.98	-0.22
		INF20-4	1	365.61	± 0.39	8.641	± 0.03	41.4	± 1.3	0.9380	± 0.0041	654.3	± 3.5	241.77	± 4.03	241.1	± 4.02	81.7	± 2.7	1.9	1.68	-0.22
			2	443.35	± 0.50	8.076	± 0.02	39.6	± 1.4	0.9319	± 0.0036	843.6	± 4.0	238.08	± 3.52	237.6	± 3.51	77.5	± 2.8	1.9	1.68	-0.22
			3	407.46	± 0.37	4.138	± 0.01	34.8	± 1.3	0.9289	± 0.0026	1508.1	± 6.3	240.25	± 2.80	239.9	± 2.80	68.6	± 2.6	1.9	1.68	-0.22
			4	573.72	± 0.55	13.719	± 0.05	32.8	± 1.3	0.9354	± 0.0051	645.0	± 4.2	248.71	± 5.30	248.0	± 5.28	66.0	± 2.8	1.9	1.68	-0.22
			5	549.40	± 0.51	17.629	± 0.07	33.0	± 1.4	0.9280	± 0.0047	476.9	± 3.0	241.42	± 4.60	240.5	± 4.59	65.0	± 2.8	1.9	1.68	-0.22
		B10-8	1	182.83	± 0.32	82.55	± 0.41	37.6	± 2.9	0.9746	± 0.0032	35.59	± 0.20	288.36	± 6.76	276.67	± 8.62	82.1	± 6.6	3.5	3.28	-0.22
			2	491.50	± 0.63	19.83	± 0.18	64.5	± 1.8	0.9447	± 0.0027	386.0	± 3.7	225.66	± 2.57	224.63	± 2.59	121.7	± 3.5	3.5	3.28	-0.22
		B10-07	1	169.25	± 0.26	4.145	± 0.021	29.8	± 2.2	0.9145	± 0.0031	615.7	± 3.7	232.39	± 3.47	231.71	± 3.46	57.4	± 4.3	3.7	3.48	-0.22
			2	214.74	± 0.33	0.3158	± 0.0084	30.9	± 1.9	0.9173	± 0.0031	10285	± 275	233.75	± 3.31	233.64	± 3.31	59.8	± 3.7	3.7	3.48	-0.22
		INF20-5	2	212.97	± 0.26	107.32	± 0.87	47.8	± 1.8	0.709	± 0.015	23.21	± 0.51	121.60	± 4.56	108.24	± 8.16	64.9	± 2.9	3.5	3.28	-0.22
			1	377.87	± 0.35	134.81	± 1.38	62.1	± 1.4	0.720	± 0.013	33.28	± 0.69	121.50	± 3.97	112.37	± 5.98	85.2	± 2.4	3.5	3.28	-0.22
		INF20-6		381.34	0.35	317.31	38.25	70.3	± 1.4	0.2480	± 0.0020	4.91	± 0.59	28.65	± 0.26	5.87	± 12.96	71.5	± 2.9	2.6	2.38	-0.22
Cala Arconte		STC22-1		988.3	± 1.1	39.128	± 0.397	55.6	± 1.5	0.8883	± 0.0016	370.0	± 3.8	194.1	± 1.3	193.10	± 1.37	96.0	± 2.6	2.3	2.08	-0.22
		STC22-2		1388.7	± 1.2	44.909	± 0.717	16.7	± 1.3	0.8392	± 0.0015	427.9	± 6.9	188.5	± 1.2	187.55	± 1.27	28.3	± 2.2	2.1	1.88	-0.22
Pozzallo		POZZ22-1		860.5	± 1.3	3.340	± 0.522	34.5	± 1.8	0.6966	± 0.0017	295.9	± 4.7	120.87	± 0.70	119.81	± 0.85	48.3	± 2.5	1.7	1.45	-0.25

Analytical errors are 2σ of the mean.
[a] $\delta^{234}U = ([^{234}U/^{238}U]_{activity} - 1) \times 1000$.
[b] $\delta^{234}U_{initial}$ corrected was calculated based on ^{230}Th age (T), i.e., $\delta^{234}U_{initial} = \delta^{234}U_{measured} X e^{\lambda 234 * T}$, and T is corrected age.
[c] $[^{230}Th/^{238}U]_{activity} = 1 - e^{-\lambda 230 T} + (\delta^{234}U_{measured}/1000)[\lambda_{230}/(\lambda_{230} - \lambda_{234})](1 - e^{-(\lambda 230 - \lambda 234) T})$, where T is the age.
Decay constants used for age calculation are available in Cheng et al. (2013).
[d] Age corrections, relative to AD 1950, were calculated using an estimated atomic $^{230}Th/^{232}Th$ ratio of 4 (± 2) x 10^{-6}.
Those are the values for a material at secular equilibrium, with the crustal $^{232}Th/^{238}U$ value of 3.8. The errors are arbitrarily assumed to be 50%
Elevation error 0.13 mDifferent colours refer to different sectors of the coast

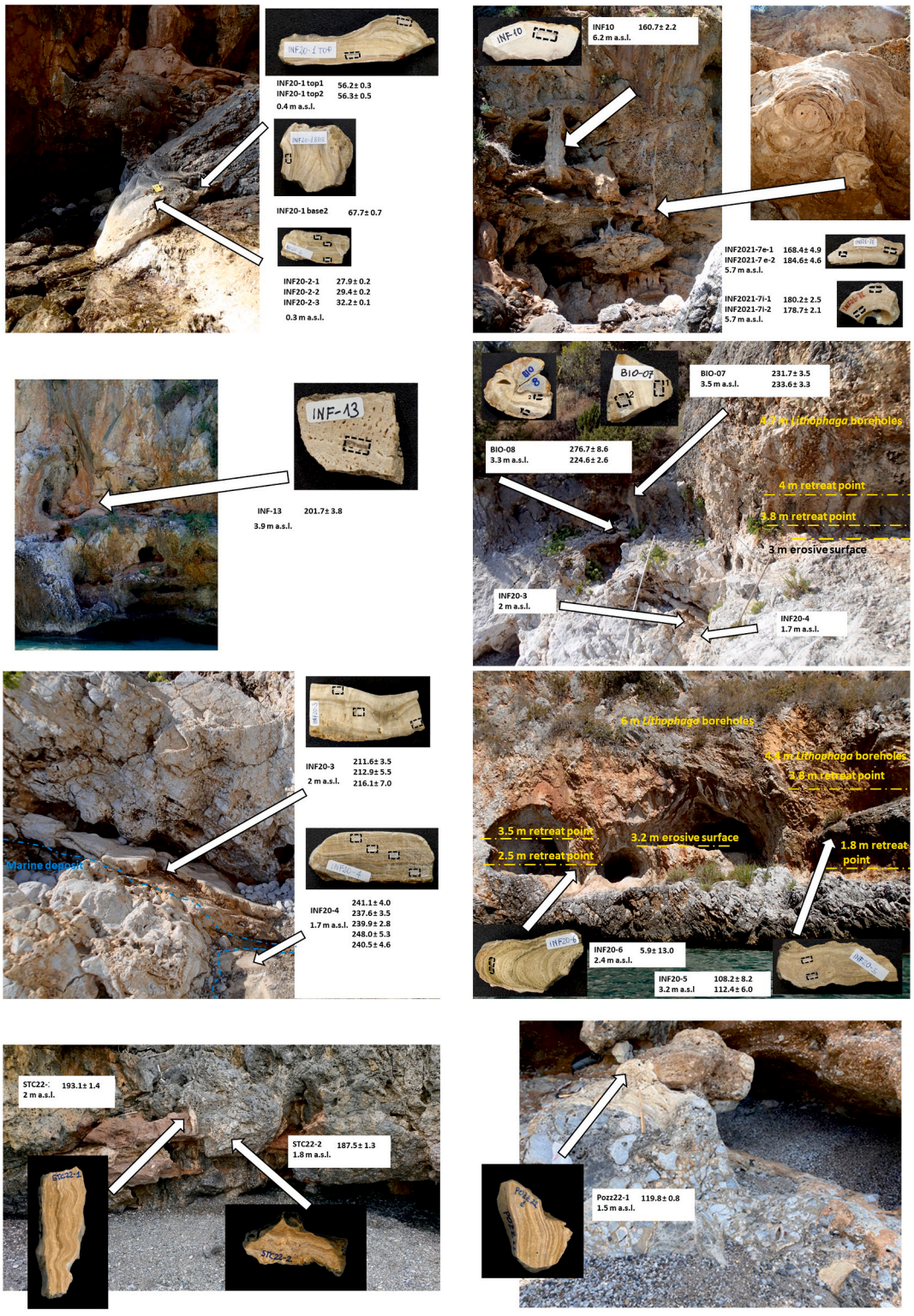

Fig. 3. Location, photo, and ages of the speleothem samples collected during this study, along with various examples of RSL indicators and their elevations. For more detailed photos see Supplementary Material S1.

dating. U/Th analyses were performed at the High-Precision Mass Spectrometry and Environment Change Laboratory (HISPEC), Department of Geosciences, National Taiwan University. All U–Th isotopic measurements were conducted on a Thermo-Finnigan Neptune multi-collector inductively coupled plasma mass spectrometer (Shen et al., 2012; Cheng et al., 2013). A gravimetrically calibrated triple-spike, ^{229}Th–^{233}U–^{236}U, and the isotope dilution method were employed to correct for mass bias and to determine U–Th isotopic compositions and contents (Cheng et al., 2013). Half-lives of U–Th nuclides used for ^{230}Th age calculation are given in Cheng et al. (2013). Uncertainties in isotopic data and ^{230}Th dates are given at the two-sigma (2σ) level or two standard deviations of the mean ($2\sigma_m$). An initial ^{230}Th/^{232}Th atomic ratio of $(4 \pm 2) \times 10^{-6}$ was applied for age correction. Table 1 shows all the analytical results.

4. Results

4.1. New stratigraphic and geomorphological data in the Baia di Infreschi

In Coral Cave, a clear upper limit of the *Lithophaga* burrow is present at 9.3 ± 0.13 m a.s.l. and is associated with an indentation corresponding to a marine notch with the retreat point measured at 8.85 ± 0.13 m a.s.l. (Fig. 4a and b). The limestone walls of the Coral Cave with *Lithophaga* boreholes are sealed by a succession of marine deposits with a bottom unit, lying on an unconformity boundary surface on the cave floor, formed by a marine conglomerate with fossils and bio-encrustations (Lithostratigraphic Unit 1, LU-1, Fig. 4a). This is followed by a complex succession of coarse sands and fine and well-rounded gravels with marine fossils and abundant remains of the corals *Cladocora caespitosa* (LU-2, Fig. 4a). This succession is overlain by aeolian cross-stratified sands (LU-3, Fig. 4a). In the inner part of the cave the described succession is covered by colluvial and partially pedogenised deposits with some layers of matrix-supported breccias (LU-4, not shown in Fig. 4a).

In other locations around the Baia di Infreschi, there is no further evidence of a clear upper limit of *Lithophaga* boreholes at ~9 m a.s.l. However, we recognized this limit along the Cilento coast, specifically at Spiaggia di Peppe (Marina di Camerota) and at Palinuro Harbour (Fig. 1), where the new measurements yielded elevations of 8.6 ± 0.1 m and 8.8 ± 0.1 a.s.l., respectively.

At Baia di Infreschi, there is no clear upper limit of *Lithophaga* boreholes, but only isolated groups of burrows are observed up to ~6 m (Figs. 3 and 5), which may indicate that the sea level has risen at least at that elevation (minimum estimated limit of the RSL highstand). However, a more continuous dense horizon of frequent burrows is present with a maximum altitude between ~4.4 and 5.9 m a.s.l. (Fig. 3), even if an unambiguous horizontal upper limit is not always identifiable. In addition, in the Baia di Infreschi, there is a succession of RSL indicators between ~4.5 and 1.7 m a.s.l. which includes cave notches, cliff notches and wave-cut surfaces (Figs. 3 and 5). Notches are well-developed and in some cases preserve *Lithophaga* burrows. In one case, a notch is sealed by gravel beach deposits. Wave-cut terraces are relatively narrow (a few

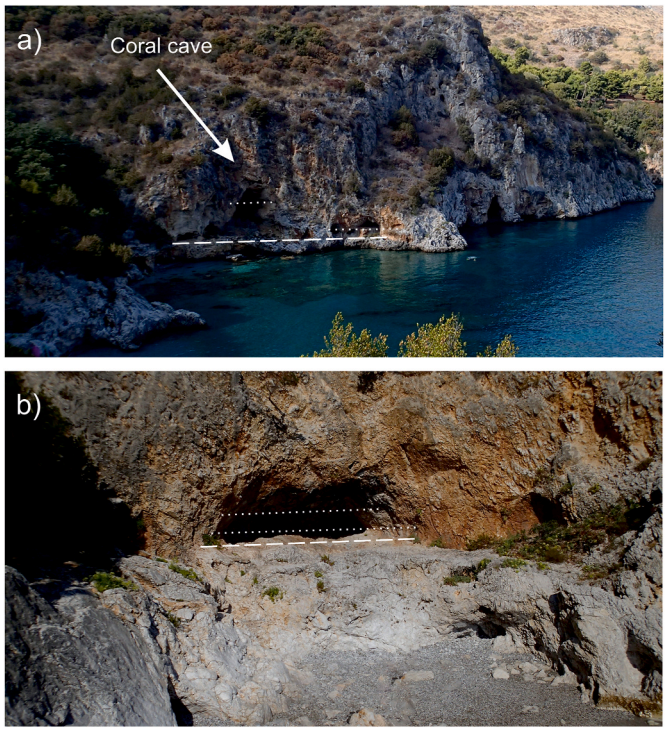

Fig. 5. Baia di Infreschi overview. a) View of Coral Cave and detected RSL indicators which include caves, cliff notches (dotted line), and wave-cut surfaces (dashed line). b) Erosive surface (dashed line) and notches (dotted lines).

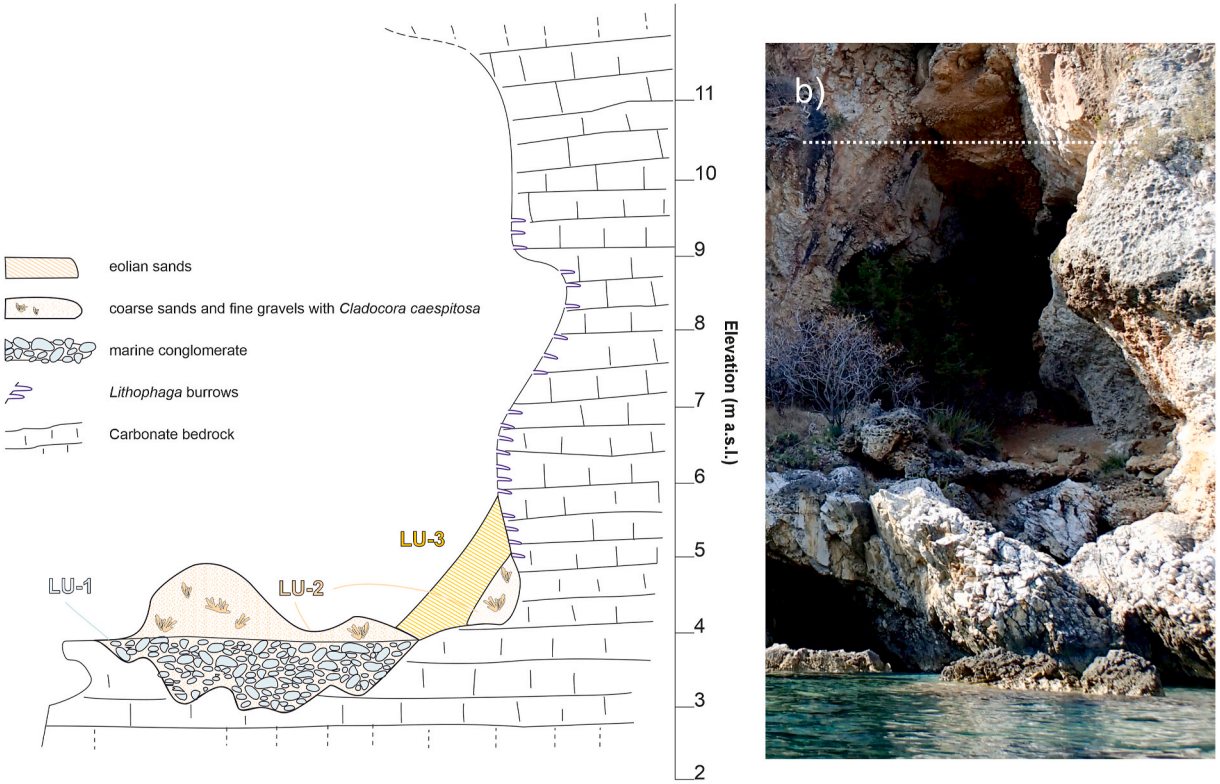

Fig. 4. Coral Cave stratigraphy. a) Lithostratigraphic Units (LU) of Coral Cave. The elevation axis is not in scale. b) Coral Cave entrance with the highlighted upper marine notch (dashed line).

metres) and are in some cases connected with marine caves or lower notch surfaces. Although there is no clear separation between these indicators, they seem to cluster in two groups, one between ~2.5 and 1.7 m a.s.l. and the other between ~4.5 and 3.5 m a.s.l. (Fig. 3).

4.2. U/Th dating

Overall, U/Th ages cover a wide temporal range between ~277 and ~6 ka (Table 1). Leaving aside the younger Holocene dating these ages appear to be distributed in three main clusters between (i) ~277 and ~160 ka (MIS 8-MIS 6); (ii) ~120 and ~108 ka (late MIS 5e-MIS 5d); and (iii) ~68 and 28 ka (MIS 4-MIS 2) (Figs. 6 and 7).

MIS 8-MIS 6 speleothems. This is the largest cluster comprising 20 out of the 30 U/Th ages performed in this study (Table 1, Figs. 6 and 7).

In the Infreschi Cave the cluster includes.

i) the two new samples from the bottom of the flowstone belonging to LU-2 without *Lithophaga* burrows at 5.7 ± 0.18 m a.s.l., which in turn cover *Lithophaga* burrows carved in the cave walls at an elevation >5.7 ± 0.18 m a.s.l., yielding ages ranging from 168.4 ± 4.9 to 184.6 ± 4.6 ka (sample INF21-7E) and from 178.7 ± 2.1 to 180.2 ± 2.5 ka (INF21–7I) (Fig. 2b and c and 7);

ii) the INF-13 sample, collected at ~3.85 m a.s.l. in the eastern sector of the Infreschi Cave, also covers a burrow generation on the cave walls, which yielded the age of 201.7 ± 3.8 ka (Figs. 3 and 7);

iii) the INF-10 sample, collected from the large column at ~6.2 m a.s.l., covering the cave wall with the *Lithophaga* burrows and yielding an age of 160.7 ± 2.2 ka (Table 1, Figs. 3, 6 and 7).

In the Baia di Infreschi near Coral Cave.

i) Samples BIO-07 (~3.5 m a.s.l.), dated between 231.7 ± 3.5 and 233.6 ± 3.3 ka and BIO-8 (~3.3 m a.s.l.) dated at 276.7 ± 8.6 and 224.6 ± 2.6 ka, which covers a marine conglomerate (Figs. 3, 6 and 7). The accuracy of the oldest age (276.7 ± 8.6 ka) needs to be considered with caution due to the possible contamination by non-authigenic ^{232}Th, considering the relative low ^{230}Th/^{232}Th (Table 1);

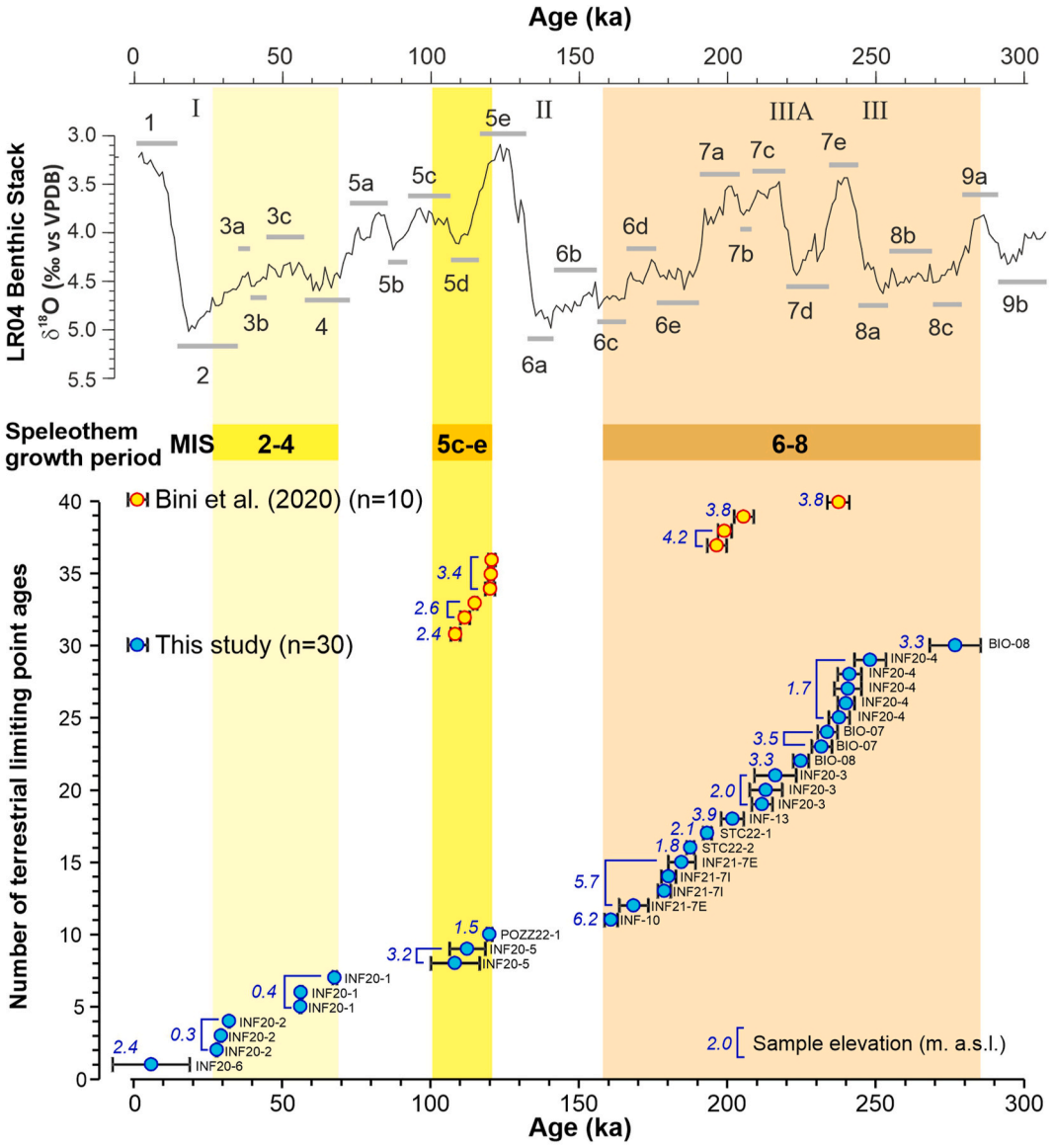

Fig. 6. Temporal distribution of the ages of the terrestrial limiting points from the Cilento coastal sites (Infreschi Cave, Baia di Infreschi and surrounding area, Fig. 1) acquired in this study and by Bini et al. (2020). showing three different periods of speleothem growth during MIS 8–6, late MIS 5e-early MIS 5c and MIS 4–2 (coloured vertical boxes). The upper panel shows the LR04 benthic δ ^{18}O stack (Lisiecki and Raymo, 2005). Grey horizontal bars highlight MIS time intervals.

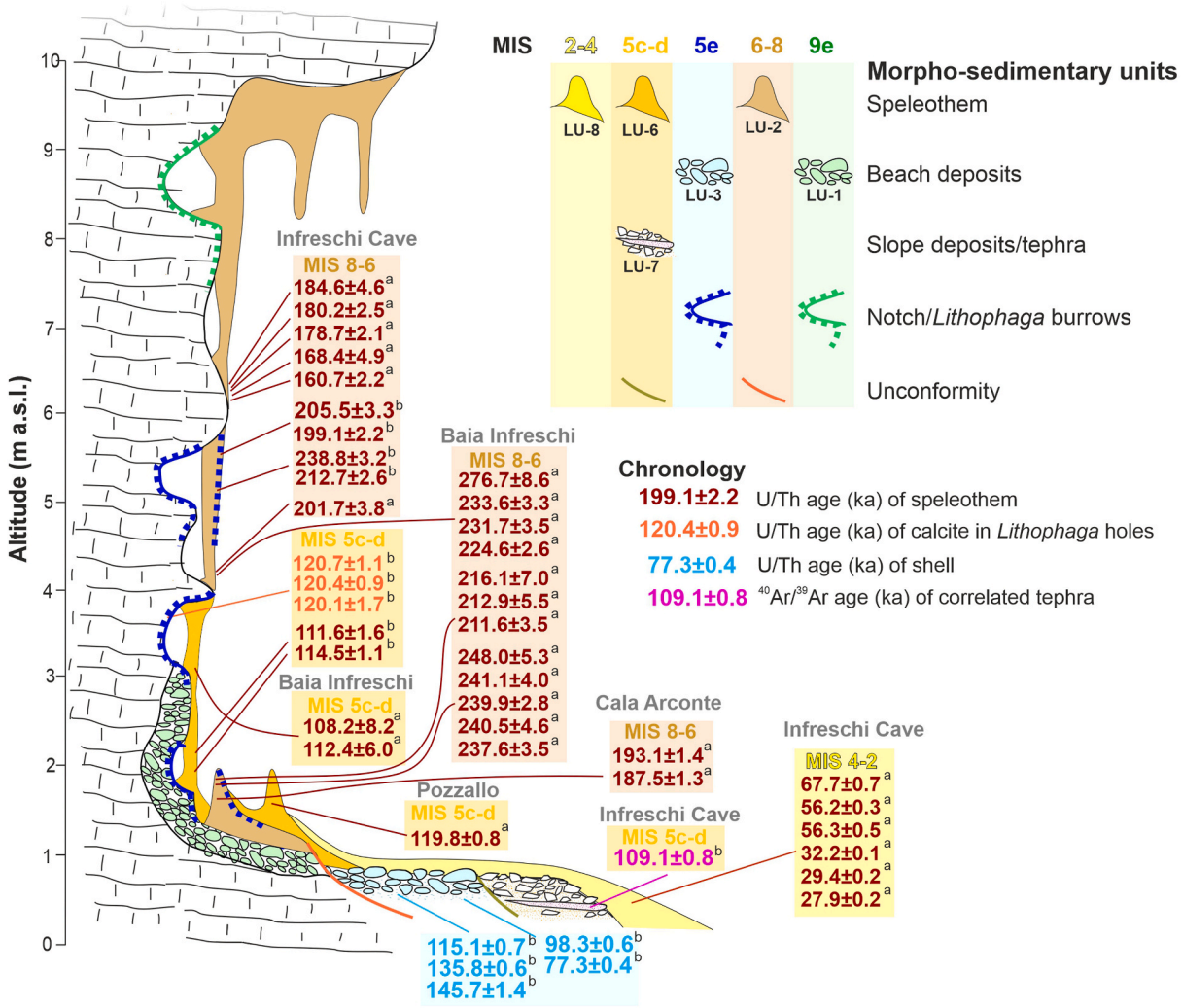

Fig. 7. Ideal composite morpho-stratigraphic section summarizing the main RSL indicators and related chronology from the Cilento coastal sites (Infreschi Cave, Baia di Infreschi and surrounding area, Fig. 1) investigated in this and in previous studies (Esposito et al., 2003; Bini et al., 2020). The elevation axis is not in scale. It is only used to allow a comprehensive view of all features. The colour-coded scheme of all reported ages indicates the type of dated material (see legend for Chronology). (a) this study and (b) Bini et al. (2020). (For interpretation of the references to colour in this figure legend, the reader is referred to the Web version of this article.)

ii) INF20-3 and INF20-4 from a second flowstone mantling a fissure filled with cemented rounded clasts (Fig. 3) at ~2 m a.s.l., yielded ages ranging from 211.6 ± 3.5 to 212.9 ± 5.5 ka and from 248.0 ± 5.3 to 237.6 ± 3.5 ka, respectively (Figs. 6 and 7, Table 1).

In Cala di Arconte beach.

i) Samples STC22-1 and STC22-2 from the eroded flowstone, again covering traces of *Lithophaga*, yielded ages between 193.1 ± 1.4 and 187.5 ± 1.3 ka (Figs. 3, 6 and 7, Table 1).

Late MIS 5e-MIS 5c speleothems. This group includes only 3 out of the 30 U/Th ages performed in this study (Table 1, Figs. 6 and 7), two from Baia di Infreschi and one from Pozzallo beach (Table 1, Figs. 3, 6 and 7).

i) Sample INF20-5 from the flowstone collected at Baia di Infreschi, which forms in a notch with a retreat point at 3.7 m a.s.l. and develops down to the lower notch covering also *Lithophaga* burrows (Fig. 3), yielded an age between ~112 and ~108 ka (Table 1);

ii) Sample POZZ22-1, a flowstone covering a marine deposit at ~1.5 m a.s.l. (Fig. 3), yielded an age of 119.8 ± 0.8 ka (Table 1, Figs. 6 and 7).

MIS 4-MIS 2 speleothems. This group includes 7 out of the 30 U/Th ages performed in this study, all collected from the flowstone (~0.3–0.4 m a.s.l.) of the Infreschi Cave, indicated as LU-8 in Fig. 2b and c (samples INF20-1, INF20-2; Fig. 3). It yielded ages ranging between ~68 and 29 ka (Table 1, Figs. 6 and 7).

Holocene speleothem. Sample INF20-6 from Baia di Infreschi yielded an imprecise and young age of 5.9 ± 13.0 ka (Table 1, Figs. 3 and 6).

5. Discussion

5.1. Reappraisal of LIG RSL at the Infreschi Cave and identification of a pre-LIG RSL highstand

5.1.1. Evidence for multiple RLS highstands

The results of the stratigraphic, morphological and geochronological investigations performed in this study, along with the literature data (Bini et al., 2020; Esposito et al., 2003), allow us to outline a more

complex history of RSL in Baia di Infreschi and in the surrounding area than previously proposed.

In the Infreschi Cave, the new U/Th ages of the flowstone-column without *Lithophaga* burrows at ~5.7 m a.s.l. date it to ~168–185 ka. This flowstone, previously undated and assumed to be part of the MIS 5 LU-6 (Bini et al., 2020), can now be associated with the generation of the MIS 6–8 flowstone (LU-2, Figs. 2 and 8), dated between ~238 and 199 ka by Bini et al. (2020). The highest *Lithophaga* burrows occurring in this MIS 6–8 generation of flowstone (LU-2) reach ~5.3 m a.s.l. (Fig. 8), and can be consequently related to the MIS 5e highstand. Therefore, the LIG highstand is constrained by the age of the burrowed speleothems, and by the age of flowstones covering the marine deposit of LU-3 and the aeolian deposit of LU-4.

This finding has a twofold consequence: (i) the RSL during the LIG highstand did not exceed the elevation of ~5.3 m a.s.l., i.e., the upper limit of the *Lithophaga* burrow generation carved into the MIS 6–8 flowstone; and (ii) the *Lithophaga* burrow limit covered by the MIS 6–8 flowstone, which in the Infreschi Cave culminates at 8.35 ± 0.18 m a.s.l. (hereafter 8.4 m), is to be referred to an older RLS highstand, preceding the MIS 8. It is important to remember that Bini et al. (2020) indicated the same limit at 8.7 m because they referred to the biological indicator, whereas we refer our measurement to the geoid. In the following sections, we discuss the implications of these findings for both MIS 5e and the older RSL highstand.

5.1.2. LIG RLS highstand and minor LIG RLS oscillations/stationing at lower elevation

The LIG RSL interpretation at the Infreschi Cave is strictly based on the *Lithophaga* burrows. The chronology is constrained by the burrowed speleothems in LU-2, by the calcite inside the *Lithophaga* burrows in LU-1, and by the speleothems covering the *Lithophaga* burrows in LU-6, dated at ~200, ~120 and ~112 ka, respectively. The highest *Lithophaga* burrows on flowstones are at 5.3 m a.s.l. and they probably represent the closest value to the maximum LIG highstand. This value agrees (within possible uncertainties) with the elevation of several sea-level indicators in the rest of Baia di Infreschi (Fig. 9). Speleothems are terrestrial limiting points and their presence indicates a time when the sea level has already dropped. We cannot provide an exact age for the LIG RSL highstand occurring at 5.3 m a.s.l., but considering the dated speleothems (Bini et al., 2020), here at ~120 ka, it had already dropped lower than ~3 m.

Notches and wave-cut terraces in the rest of the bay are located at lower elevations, indicating phases of temporary sea-level standstills during its progressive lowering (Fig. 9). These phases are constrained by the age of the INF20-5 flowstone, which departs from a notch with a retreat point at 3.7 m a.s.l. and develops down to the lower notch also covering *Lithophaga* burrows (Fig. 3). Despite a relative high age uncertainty due to detrital contamination, the sample yielded an age between ~112 and 108 ka (Table 1), constraining the development of the sea-level markers within the MIS 5e. The attribution of all the marine indicators between ~6 m a.s.l. and the present sea level to the LIG is also consistent with the preservation of continental deposits (LU-7) with Mousterian artefacts and the tephra layer of the X-6 tephra (~109 ka; Bini et al., 2020; Zanchetta et al., 2018) at the Infreschi Cave, as well as in other caves along the Cilento coast (e.g., Spagnolo et al., 2024), close to the present-day sea level. This succession of continental deposits (LU-7) is then covered by the MIS 4-MIS 3 generation of flowstone in the western sector of the cave (LU-8, Fig. 2b and c), here dated from 67.7 ± 0.7 to 27.9 ± 0.2 ka (samples INF20-1 and INF-20-2, Figs. 3 and 7, Table 1).

Overall, this indicates the absence of any further sea transgression above present-day sea level during subsequent MIS 5 sub-stages. During MIS 5e, at the Baia di Infreschi, there was an early highstand close to ~5.3 m a.s.l. Its termination is well constrained before 120 ka (Bini et al., 2020), while its beginning is not well defined. This highstand is followed by some standstills/oscillations which seem to cluster between ~4.5 and 3.0 m and 2.5–1.7 m a.s.l. (Fig. 9). According to the U/Th dating obtained by Bini et al. (2020), these oscillations terminated

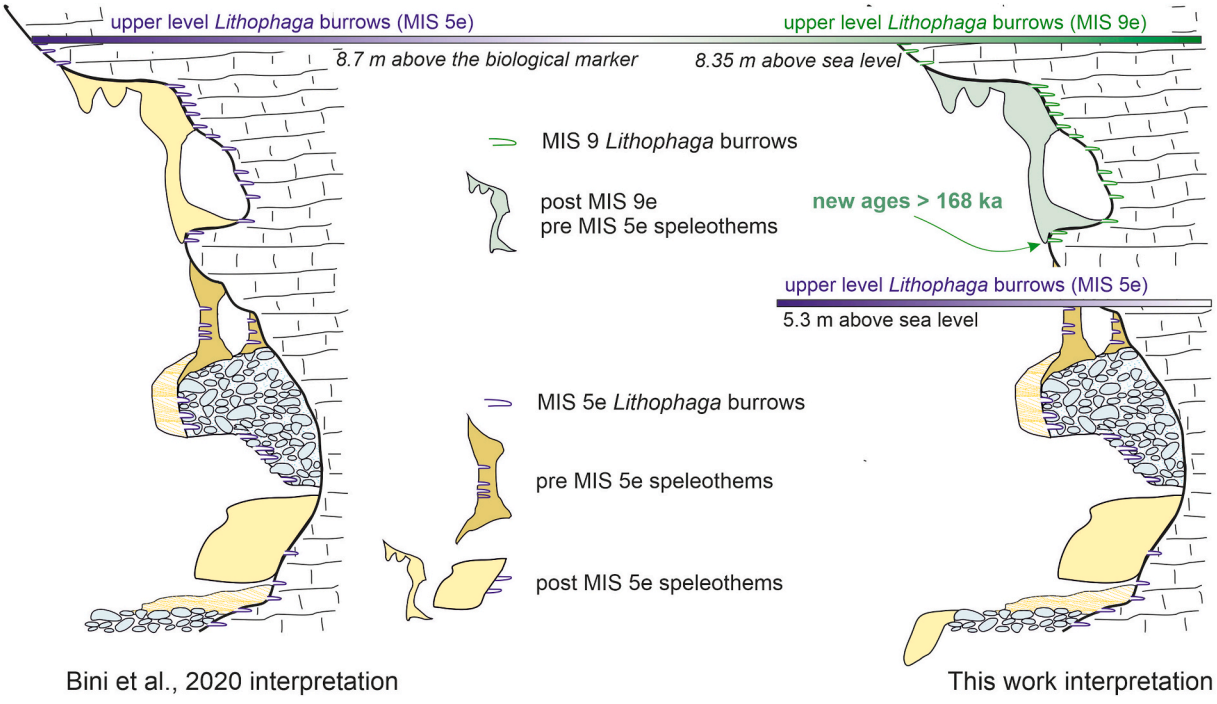

Fig. 8. Comparison between the interpretation of Bini et al. (2020, left panel) and the findings of this study (right panel) in the context of the MIS 5/MIS 9 highstand at the Infreschi Cave. Note the new age of ca. 160 ka at the base of the highest non-burrowed speleothem which covers Lithophaga traces on the rock. These imply the presence of two distinct generations of Lithophaga burrows. The older generation, characterized by a straight line at about 8.4 m a.s.l., can plausibly be attributed to MIS 9e. Meanwhile, the younger generation, visible up to 5.3 m a.s.l., is associated with MIS 5e. In Bini et al. (2020), the upper limit of Lithophaga burrows (8.7 m) is referred to the biological marker, while the measurement of the same limit conducted in this study (8.4 m) is referred to the ITALGEO2005 geoid.

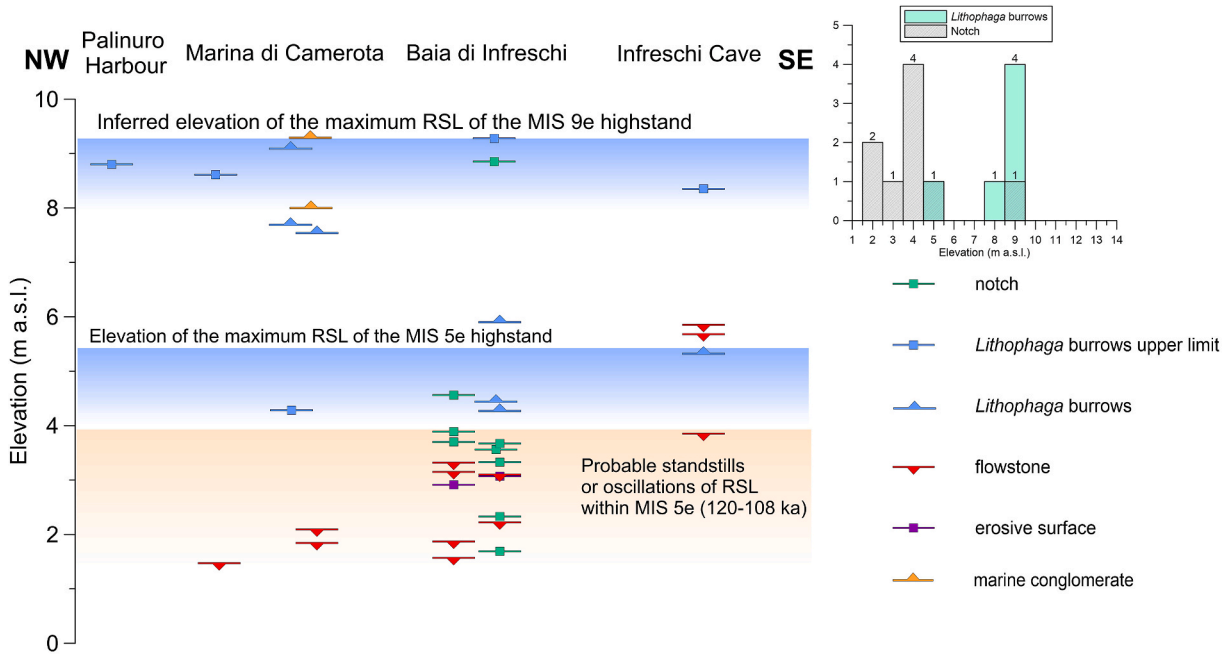

Fig. 9. RLS data. The main graph illustrates the altitudinal distribution and associated ages of the RSL indicators along the Palinuro - Infreschi coast. In the upper right corner, a vertical bar chart shows the distribution of the upper limit elevations of the Lithophaga burrows and of the notch elevations. The elevations of RLS during MIS 9e and MIS 5e are highlighted in light blue, and probable MIS 5e oscillations are highlighted in light orange. (For interpretation of the references to colour in this figure legend, the reader is referred to the Web version of this article.)

before ~120 ka when the deposition of flowstones within LU-6 started (Fig. 2a and b). This is also confirmed by the age of the INF20-5 speleothem deposition and of the Pozzallo beach flowstone, (sample POZZ22-1), located at only 1.5 m a.s.l. (Figs. 3 and 7), yielding an age of 119.8 ± 0.8 ka (Table 1). Notably, the Pozzallo flowstone is at an elevation substantially lower than the speleothem of the Infreschi Cave dated by Bini et al. (2020) to ~121–120 ka (~3.70 m a.s.l.), thus providing evidence that at ~120 ka the LIG RLS had already fallen below 1.5 m a.s.l (Fig. 7). According to our chronology the LIG highstand ended before 120 ka lasting less than 9 kyr. As a consequence, the intra-LIG sea-level standstills, of necessity, have to be relatively short events. This is also in agreement with a recent study at Guattari Cave (Rolfo et al., 2023) and "Grotta delle Capre" (Giaccio et al., 2024), along the Tyrrhenian coast ~200 km NE of the Infreschi Cave. Here speleothem evidences indicate that the LIG RSL was less than 3 m a.s.l. as early as before 123 ka, while afterwards it no longer rose above this elevation. In summary, the U/Th chronology from speleothem terrestrial limiting points does not precisely determine the age of the maximum LIG RSL at ~5.3 m a.s.l., nor does it determine the age of the following minor oscillations/stationing at lower elevations. However, it provides compelling evidence that these events occurred during the LIG. It also indicates that by 120 ka, or possibly earlier, RSL was lower than 1.5 m a.s.l. The detected short duration of the LIG RSL highstand being characterized by multiple oscillations well aligns with the isotopic-based RSL curve proposed by Rohling et al. (2019). Indeed it documents several oscillations in the global sea level from ~129 ka to ~122 ka ultimately falling to the present level at ~120 ka. The highstand at ~5.3 m a.s.l. is also partially consistent with a suite of predicted RSL curves by the GIA model using ICE-6G ice-sheet input data and VM2 mantle viscosity profile (Peltier et al., 2015) performed by Bini et al. (2020), who indicate a maximum local RSL of ~4 m. The ~1.3 m difference can be related to model inaccuracies but also to a possible small tectonic uplift (in this case <0.01 mm/yr). This confirms a relatively stable tectonic condition of the Cilento coast, as suggested by Ferranti et al. (2006).

5.1.3. *Pre-LIG, MIS 9e RSL highstand*

The elevation of the older RSL highstand, recognized at Infreschi Cave at 8.4 ± 0.18 m a.s.l., is comparable with the upper level of *Lithophaga* burrows at Coral Cave (9.3 ± 0.13 m a.s.l.) and with the related notch at 8.85 ± 0.13 m a.s.l. A sub-horizontal upper limit of *Lithophaga* burrows having an altitude close to ~8–10 m a.s.l. is also reported in other sectors of the Cilento coast (Bini et al., 2020) and documented in this study at Spiaggia di Peppe (Marina di Camerota, 8.6 ± 0.1 m a.s.l.) and Palinuro Harbour (8.8 ± 0.1 m a.s.l.) (Figs. 1 and 9). This indicates that the *Lithophaga* upper level can be discontinuously followed for several kilometres along the coast with a relatively small difference in altitude, also suggesting no significant tectonic displacements in the area.

In addition to the above discussed stalagmite evidence in the Infreschi Cave, the occurrence of an RSL highstand predating the LIG is further supported by U/Th dating of other speleothems covering burrows and/or beach deposits collected both in the Infreschi Cave (sample INF13, ~3.85 m a.s.l 201.7 ± 3.8 ka, INF20-3, ~2 m a.s.l., 211.6 ± 3.5–212.9 ± 5.5 ka.), in Baia di Infreschi (BIO-07, ~3.5 m a.s.l., 231.7 ± 3.5 ka-233.6 ± 3.3 ka, BIO-8, ~3.3 m a.s.l., 276.7 ± 8.6–224.6 ± 2.6 ka) and along the Marina di Camerota coast at Cala di Arconte beach (samples STC22-1 and STC22-2, ~2 m a.s.l., 193.1 ± 1.4–187.5 ± 1.3 ka) (Figs. 3, 6 and 7, Table 1). Overall, the ages of the MIS 8-6 speleothem generation continuously cover the entire interval of MIS 7 (Fig. 6), thus providing strong evidence that in this area the RSL during MIS 7 never reached the present sea level, or at least not above ~2 m a.s.l. (Table 1). This is consistent with data presented from the Argentarola marine cave (Bard et al., 2002) and with the recent reconstruction of the nearby margin of northern Calabria (Cerrone et al., 2021b), even if this latter reconstruction is indirect, based on restoring RSL indicators assuming a different uplift rate. In general, this agrees with regional to global models indicating that the MIS 7 RSL highstand was lower than the MIS 9, MIS 5 and Holocene highstands (e.g., Bintanja et al., 2005; Grant et al., 2014).

The chronology of the speleothems at the Infreschi Cave and other investigated localities (Fig. 10), as well as the global RSL models (e.g.,

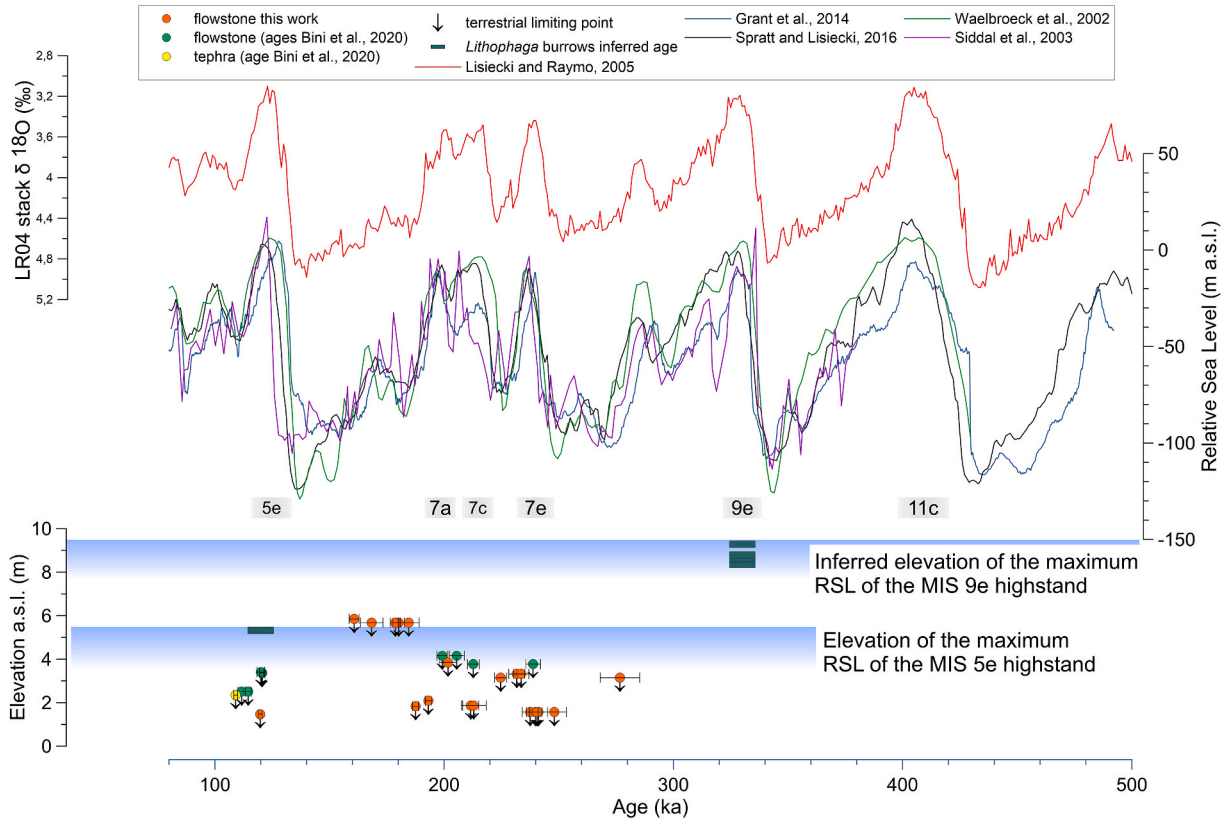

Fig. 10. *RLS over the last ~300 kyrs. From the top: $\delta^{18}O$ variation in LR04 marine stack (red line, Lisiecki and Raymo, 2005), Relative Sea Level curves (blue line Grant et al., 2014; green line Waelbroeck et al., 2002; black line Spratt and Lisiecki, 2016; purple line Siddall et al., 2003). Elevation and ages (2σ error) of terrestrial limiting points (flowstones) from Bini et al. (2020, green points) and the findings of this study (orange points). Elevation (inferred ages) of Lithophaga burrows (green boxes). The inferred elevations of RLS during MIS 9e and MIS 5e are highlighted in light blue.* (For interpretation of the references to colour in this figure legend, the reader is referred to the Web version of this article.)

Grant et al., 2014), would indicate the MIS 9e RSL highstand as the most probable for correlating to the upper level of the *Lithophaga* burrows at ~9 m a.s.l. This aligns with the presence in the Cilento area of continental successions containing Lower Paleolithic artefacts with handaxes (e.g., Gambassini and Palma di Cesnola, 1972). These continental successions lying on a terrace at ~20–40 m a.s.l., probably of marine origin (e.g. Esposito et al., 2003; Carmignani et al., 2021), are attributed to MIS 11 (Carmignani et al., 2021), predating the cliff where the upper level of the *Lithophaga* burrows at ~9 m a.s.l was formed. Therefore, assuming that these higher marine morphologies and sedimentary successions correspond to MIS 11, the RSL highstand at ~9 m a.s.l. need to be consequently associated with the MIS 9e RSL highstand.

5.2. Implications for the regional LIG and MIS 9e RSL and uplift rate

The reconstruction proposed in this work indicates that MIS 9e sea-level indicators are approximately 3 m higher than MIS 5e indicators. Regionally, the RSL level deviates from the global eustatic sea level, for instance, for the GIA (e.g., Creveling et al., 2015; Antonioli et al., 2018, Stocchi et al., 2018) and the effect of the local tectonic (e.g., Cerrone et al., 2021b; Antonioli et al., 2018). Estimates suggest that during MIS 5e, eustatic sea levels were probably between 2 and 9 m higher than present (e.g., Siddall et al., 2003; Hearty et al., 2007; Waelbroeck et al., 2002; Kopp et al., 2009; Dutton et al., 2015; Polyak et al., 2018; Dyer et al., 2021, Fig. 9). In the Central Mediterranean region and along the Italian Tyrrhenian coast in stable tectonic areas, the LIG highstand is estimated to be around +6 ± 3 m a.s.l. (e.g., Ferranti et al., 2006; Antonioli et al., 2018). Elevation data for the MIS 9e highstand are scarce and obtained through different approaches, showing varying differences between MIS 9e and MIS 5e sea levels. The lack of reliable dated sea-level markers for MIS 9e in the Mediterranean, particularly in the southern Tyrrhenian Sea, presents challenges in understanding past sea-level changes. Recently, in the more tectonically stable Apulia region, Pieruccini et al. (2022) have reported a succession of notches associated with *Lithophaga* burrows in the Romanelli Cave (Fig. 1) at 9.2 ± 0.2 m a.s.l. and 7 ± 0.20 m a.s.l. covered by flowstones. Their U/Th dating allowed the attribution of both to MIS 9. In the same work, a lower notch at 5.5 ± 0.20 m a.s.l. was instead correlated to the MIS 5e RSL highstand. Sites like Romanelli Cave and Baia di Infreschi provide insights into the elevation of the sea level during MIS 9e, both potentially indicating that other sites revealing evidence of the MIS 9e highstand can be found and chronologically constrained in the future.

5.3. Implication for the local stratigraphy of the archaeological caves

Several archaeological caves in the area show stratigraphic evidence of two distinct marine deposits, and their chronology can be reevaluated in the light of our data. For instance, at the shelter and the cave of Poggio, Boscato et al. (2009) (Fig. 1) describe a succession with a marine conglomerate up to 9.5 m a.s.l., followed by a continental succession containing Paleolithic artefacts. A level ~6 m above the top of the marine conglomerate (Level 16, Boscato et al., 2009) was dated at 111.8 ± 9.5 ka by thermo-luminescence technique. Subsequently, the basal marine layer was suggested to correlate to one of the sea-level highstands during MIS 7 (Boscato et al., 2009). At Grotta di Scario, Ronchitelli et al. (1998, 2011) (Fig. 1) identified two sedimentary successions, separated by an erosive surface. The lower one is characterized by a basal marine conglomerate containing *Cladocora caespitosa* and *Spondylus* sp. and, according to Ronchitelli et al. (2011), it corresponds to an upper limit of the *Lithophaga* burrow at 13 m a.s.l. This

marine-to-continental succession was tentatively correlated with MIS 6–7. A second marine transgression eroded this level, leaving a beach deposit containing specimens of *Thetystrombus latus* (*Strombus bubonius* in Ronchitelli et al., 2011) supporting that the deposition occurred during the highstand phase of the LIG (Gambassini and Ronchitelli, 1998; Ronchitelli et al., 2011). The dated speleothems in the area of Baia di Infreschi and Cala di Arconte indicate that the RSL during MIS 7 is below ~2 m a.s.l. and this implies that the infillings of the Poggio and Scario caves are potentially much older than those supposed so far. Thus, the marine deposits/markers cannot be correlated with the MIS 7 highstand, but they should be correlated with an older interglacial highstand. We suggest that these levels should correspond to MIS 9e.

In general, marine conglomerates are not considered precise indicators of RSL (Kellett et al., 2014; Rovere et al., 2016). Therefore, the Grotta del Poggio deposit, even if its elevation is close to the measured upper level of *Lithophaga* burrows in different parts of the coast and correlated by us with the MIS 9e highstand, should be approached with caution. Whereas the upper limit of the *Lithophaga* burrows in the Grotta di Scario is a more accurate indicator of the RSL, it is noteworthy that the elevation of the upper limit of the *Lithophaga* at Scario is higher than those measured in the areas of Marina di Camerota and Baia di Infreschi. The difference in elevation could be reasonably attributed to an increased tectonic component, probably influenced by the Calabrian arc subduction system, as one moves southward from Camerota (e.g. Ferranti et al., 2006; Facenna et al., 2013; Cerrone et al., 2021b).

6. Concluding remarks

Our investigations revealed the presence of two main sets of RSL indicators in the Baia di Infreschi, at two different elevations: (i) an upper set, which includes a notch and the upper limit of *Lithophaga* boreholes, ranges between ~8.4 and 9.3 m a.s.l. (Figs. 8 and 9); and a (ii) lower set, which in turn includes a series of RSL oscillations (*Lithophaga* burrows, notches, erosive surfaces) clustering at the elevations of ~5.3 m, ~4.5–3.0 m, and 2.5–1.7 m a.s.l.

The upper set of sea-level indicators is covered by a drapery of speleothems dated by U/Th between ~160 and ~280 ka (MIS 6 to late MIS 8), which constrains their attribution to the MIS 9e highstand. The recognition of these morphological features at the same elevation for ~12 km along the Cilento coast suggests a relatively uniform tectonic activity with no major relative displacements. This allows us to use the upper set of RSL indicators as a marker of the MIS 9e, in order to assess or re-assess the age of local sedimentary-archaeological successions and paleo-morphologies, like those of the marine levels previously correlated with MIS 7 highstands, which should now be related to MIS 9e.

The lower group of sea-level indicators, which are imprinted in speleothems dated between ~180 and 230 ka (MIS 8-MIS 6) and are covered with speleothems dated between ~120 and 60 ka, are instead attributed to the LIG RSL highstand. The multiple indicators at elevations ranging between ~5.3 m, ~4.5–3.0 m and 2.5–1.7 m a.s.l. indicate a complex dynamic of the LIG RLS, characterized by several oscillations before its definitive fall below the present sea level at ~120 ka. This calls for caution when attributing morphological and sedimentary indicators, which are lower than the local indicators of the LIG highstand, to oscillations that possibly occurred during subsequent MIS 5 substages (e.g., MIS 5c and MIS 5a).

As a matter of fact, according to the U/Th ages available, there are no evident traces of RSL marine indicators above the present sea level after ~120 ka.

The data presented in this work and the recently published data from the Grotta Romanelli in Puglia suggest that there is more than occasional evidence of the MIS 9e highstand along the Italian coast. Such evidence calls for a potential reconsideration of other study-sites where high-elevation markers have been, without robust geochronological constraints, correlated to the LIG.

CRediT authorship contribution statement

Ilaria Isola: Writing – review & editing, Writing – original draft, Methodology, Investigation, Data curation, Conceptualization. **Monica Bini:** Writing – review & editing, Writing – original draft, Investigation, Funding acquisition, Data curation, Conceptualization. **Andrea Columbu:** Writing – review & editing, Writing – original draft. **Mauro Antonio Di Vito:** Investigation, Conceptualization. **Biagio Giaccio:** Writing – review & editing, Writing – original draft, Investigation, Conceptualization. **Hsun-Ming Hu:** Formal analysis. **Fabio Martini:** Investigation, Conceptualization. **Francesca Pasquetti:** Writing – review & editing, Writing – original draft, Data curation, Conceptualization. **Lucia Sarti:** Investigation, Conceptualization. **Federica Mulè:** Data curation. **Antonio Mazzoleni:** Data curation. **Chuan-Chou Shen:** Writing – review & editing, Formal analysis. **Giovanni Zanchetta:** Writing – review & editing, Writing – original draft, Investigation, Funding acquisition, Data curation, Conceptualization.

Declaration of competing interest

The authors declare that they have no known competing financial interests or personal relationships that could have appeared to influence the work reported in this paper.

Data availability

Data will be made available on request.

Acknowledgements

This manuscript is dedicated to the memory of Gennaro (Rino) Scarano, who supported in different ways our research, to his family, and to all the staff of the Campeggio Village Romano (Marina di Camerota). We wish to thank the local Port Authority, the Municipality of Camerota, the Parco del Cilento e Vallo di Diano and the Soprintendenza Archeologica for making this research possible. Part of this research was supported by the project 'FUcino Tephrochronology Unites quaternary REcords (FUTURE)', supported by the Italian Ministry of Education, University and Research (grant PRIN no. 20177TKBXZ_003; G. Zanchetta, coordinator). U/Th dating was supported by grants from the Ministry of Science and Technology (MOST) and National Science and Technology Council, Taiwan, ROC (110-2123-M-002-009 and 111-2116-M-002-022-MY3 to C.-C.S.), the Higher Education Sprout Project of the Ministry of Education, Taiwan, ROC (110L901001 to C.-C.S.), the National Taiwan University (112L894202 to C.-C.S.). GZ and MB are funded by the University of Pisa, through "Ateneo Funding".

Appendix A. Supplementary data

Supplementary data to this article can be found online at https://doi.org/10.1016/j.qsa.2024.100212.

References

Antonioli, F., Oliverio, M., 1996. Holocene sea-level rise recorded by a radiocarbon-dated mussel in a submerged speleothem beneath the Mediterranean Sea. Quat. Res. 45, 4–4.

Antonioli, F., Anzidei, M., Lambeck, K., Auriemma, R., Gaddi, D., Furlani, S., Surace, L., 2007. Sea-level change during the Holocene in Sardinia and the northeastern Adriatic (central Mediterranean Sea) from archaeological and geomorphological data. Quat. Sci. Rev. 26 (19–21), 2463–2486.

Antonioli, F., Presti, V.L., Rovere, A., Ferranti, L., Anzidei, M., Furlani, S., Vecchio, A., 2015. Tidal notches in Mediterranean Sea: a comprehensive analysis. Quat. Sci. Rev. 119, 66–84.

Antonioli, F., Ferranti, L., Stocchi, P., Deiana, G., Lo Presti, V., Furlani, S., Marino, C., Orru, P., Scicchitano, G., Trainito, E., Anzidei, M., Bonamini, M., Sansò, P., Mastronuzzi, G., 2018. Morphometry and elevation of the last interglacial tidal notches in tectonically stable coasts of the Mediterranean Sea. Earth Sci. Rev. 185, 600–623.

Ascione, A., Romano, P., 1999. Vertical movements on the eastern margin of the Tyrrhenian extensional basin. New data from Mt. Bulgheria (Southern Apennines, Italy). Tectonophysics 315, 337–356.
Ascione, A., Caiazzo, C., Hippolyte, J.C., Romano, P., 1997. Pliocene-Quaternary extensional tectonics and morphogenesis at the eastern margin of the southern tyrrhenian basin (Mt. Bulgheria, Campania, Italy). Il Quat. 10, 571–578.
Asioli, A., Capotondi, L., Sironi, M.B.C., 2005. The Tyrrhenian stage in the Mediterranean: definition, usage and recognition in the deep-sea record. A proposal. Rendiconti dei Lincei 16, 297–310.
Bard, E., Antonioli, F., Silenzi, S., 2002. Sea-level during the penultimate interglacial period based on submerged stalagmite from Argentarola Cave (Italy). Earth Planet Sci. Lett. 196 (3– 4), 135–146.
Bini, M., Isola, I., Pappalardo, M., Ribolini, A., Favalli, M., Ragaini, L., Zanchetta, G., 2014. Abrasive notches along the Atlantic Patagonian coast and their potential use as sea level markers: the case of Puerto Deseado (Santa Cruz, Argentina). Earth Surf. Process. Landforms 39 (11), 1550–1558.
Bini, M., Isola, I., Zanchetta, G., Pappalardo, M., Ribolini, A., Ragaini, L., Baroni, C., Boretto, G., Fuck, E., Morigi, C., Salvatore, M.C., Bassi, D., Marzaioli, F., Terrasi, F., 2018. Middle Holocene relative sea-level along atlantic Patagonia: new data from Camarones (Chubut, Argentina). Holocene 28, 56–64.
Bini, M., Zanchetta, G., Drysdale, R.N., Giaccio, B., Stocchi, P., Vacchi, M., Hellstrom, J. C., Couchoud, I., Monaco, L., Ratti, A., Martini, F., Sarti, L., 2020. An end to the last interglacial highstand before 120 ka: relative sea-level evidence from Infreschi cave (southern Italy). Quat. Sci. Rev. 250, 106658.
Bintanja, R., Van De Wal, R.S., Oerlemans, J., 2005. Modelled atmospheric temperatures and global sea levels over the past million years. Nature 437 (7055), 125–128.
Boscato, P., Boschian, G., Caramia, F., Gambassini, P., 2009. Il Riparo del Poggio a Marina di Camerota (Salerno): culture e ambiente, LIX. Rivista di Scienze Preistoriche, pp. 5–40.
Carmignani, L., Martini, I., Spagnolo, V., Dominici, C., Rossini, M., Scaramucci, S., Moroni, A., 2021. Middle and early upper pleistocene human occupations in southern Italy. A reassessment of the assemblages from Cala d'Arconte, Capo Grosso and Cala Bianca. J. Archaeol. Sci.: Reports 40, 10325.
Carobene, L., 2015. Marine Notheces and sea-cave bioerosional grooves in microtidal areas: examples from the tyrrhenian and Ligurian coasts-Italy. J. Coast Res. 31, 536–556.
Cerrone, C., Ascione, A., Robustelli, G., Tuccimei, P., Soligo, M., Balassone, G., Mormone, A., 2021b. Late Quaternary uplift and sea level fluctuations along the Tyrrhenian margin of Basilicata - northern Calabria (southern Italy): new constraints from raised paleoshorelines. Geomorphology 395, 107978.
Cerrone, C., Vacchi, M., Fontana, A., Rovere, A., 2021a. Last Interglacial sea-level proxies in the western Mediterranean. Earth Syst. Sci. Data 13, 4485–4527.
Cheng, H., Lawrence, Edwards R., Shen, C.C., Polyak, V.J., Asmerom, Y., Woodhead, J., Hellstrom, J.H., Wang, Y., Kong, X., Spötl, C., Wang, X., Calvin, A.E., 2013. Improvements in ^{230}Th dating, ^{230}Th and ^{234}U half-life values, and U-Th isotopic measurements by multi-collector inductively coupled plasma mass spectrometry. Earth Planet Sci. Lett. 371–372, 82–91.
Columbu, A., Calabrò, L., Chiarini, V., De Waele, J., 2021. Stalagmites: from science application to museumization. Geoheritage 13, 1–11.
Creveling, J.R., Mitrovica, J.X., Hay, C.C., Austerm, J., Kopp, R.E., 2015. Revisiting tectonic corrections applied to Pleistocene sea-level highstands. Quat. Sci. Rev. 111, 72–80.
De Waele, J., D'Angeli, I.M., Bontognali, T., Tuccimei, P., Scholz, D., Jochum, K.P., Columbu, A., Bernasconi, F., Fornos, J., Gonzalez, E., Tisato, N., 2018. Speleothems in a north Cuban cave register sea-level changes and Pleistocene uplift rates. Earth Surf. Process. Landforms 43 (11), 2313–2326.
Dumitru, O.A., Polyak, V.J., Asmerom, Y., Onac, B.P., 2021. Last interglacial sea-level history from speleothems: a global standardized database Oana. Earth Syst. Sci. Data 13, 2077–2094, 2021.
Dutton, A., Lambeck, K., 2012. Ice volume and Sea Level during the last interglacial. Science 337, 216–219.
Dutton, A., Carlson, A.E., Long, A.J., Milne, G.A., Clarck, P.U., De Conto, R., Horton, B.P., Rahmstorf, S., Raymo, R.E., 2015. Sea-level rise due to polar ice-sheet mass loss during past warm periods. Science 349 (6244), aaa4019.
Dyer, B., Austermann, J., D'Andrea, W.J., Creel, R.C., Sandstrom, M.R., Cashman, M., Rovere, A., Raymo, M.E., 2021. Sea-level trends across the Bahamas constrain peak last interglacial ice melt. Proc. Natl. Acad. Sci. USA 17 (33), 118.
Esat, T.M., McCulloch, M.T., Chappell, J., Pillans, B., Omura, A., 1999. Rapid fluctuations in sea level recorded at Huon Peninsula during the penultimate deglaciation. Science 283, 197–201.
Esposito, C., Filocamo, F., Marciano, R., Romano, P., Santangelo, N., Scarciglia, F., Tuccimei, P., 2003. Late-Quaternary shorelines in southern Cilento (Mt. Bulgheria): moprhostratigraphy and chronology. Il Quat. 16, 3–14.
Facenna, C., Becker, T.W., Aurer, K., Billi, A., Boschi, L., Brun, J.P., Capitanio, F.A., Funiciello, F., Horvàth, F., Jolivet, K., Piromallo, C., Royden, K., Rossetti, F., Serpelloni, E., 2013. Mantle dynamics in the Mediterranean. Rev. Geophys. 52, 283–332. https://doi.org/10.1002/2013RG000444.
Ferranti, L., Antonioli, F., Mauz, B., Amorosi, A., Dai, Pra G., Mastronuzzi, G., Monaco, C., Orrù, P., Pappalardo, M., Radke, U., Renda, P., Romano, P., Sansò, P., Verrubbi, V., 2006. Markers of the last interglacial sea-level high stand along the coast of Italy: tectonic implications. Quat. Int. 145–146, 30–54.
Gambassini, P., Palma di Cesnola, A., 1972. Notizie sui giacimenti acheuleani delle dune fossili di Marina di Camerota (Salerno). In: Atti XIV Riunione Scientifica Dell. 'Istituto Italiano di Preistoria e Protostoria, pp. 147–174.
Gambassini, P., Ronchitelli, A., 1998. Linee di sviluppo dei complessi del Paleolitico inferiore-medio nel Cilento, XLIX. Rivista di Scienze Preistoriche, pp. 357–378.
Giaccio, G., Bini, M., Isola, I., Hu, H.-M., Rolfo, M.F., Shen, C.-C., Ferracci, A., Monaco, L., Pasquetti, F., Zanchetta, G., 2024. Constraining the end of the Last Interglacial (MIS 5e) relative sea level highstand in central Mediterranean: new data from Grotta delle Capre, central Italy. Global Planet. Change. https://doi.org/10.1016/j.gloplacha.2023.104321.
Govin, A., Capron, E., Tzedakis, P.C., Verhyden, S., Ghaleb, B., Hillaire-Marcel, C., St-Onge, G., Stoner, J.S., Bassinot, F., Bazin, L., Blunier, T., Combourieu-Nebout, N., El Quahabi, A., Genty, D., Gersonde, R., Jimenez-Amat, P., Landais, A., Martrat, B., Masson-Delmotte, V., Perrenin, F., Seidenkrantz, M.-S., Veres, D., Waelbroeck, C., Zahn, R., 2015. Sequence of events from the onset to the demise of the Last Interglacial: evaluating strengths and limitations of chronologies used in climatic archives. Quat. Sci. Rev. 129, 1–36.
Grant, K.M., Rohling, E.J., Bronk Ramsey, C., Cheng, H., Edwards, R.L., Florindo, F., Heslop, D., Marra, F., Roberts, A.P., Tamisiea, M.E., Williams, F., 2014. Sea-level variability over five glacial cycles. Nat. Commun. 5, 5076.
Hearty, P.J., Miller, G.H., Stearns, C., Szabo, B.J., 1986. Aminostratigraphy of Quaternary shorelines around the Mediterranean basin. Geol. Soc. Am. Bull. 97, 850–858.
Hearty, P.L., Hollin, J.T., Neumann, A.C., O'Leary, M.J., McCulloch, M., 2007. Global sea-level fluctuations during the Last Interglaciation (MIS5e). Quat. Sci. Rev. 26, 2090–2112.
Hillaire-Marcel, C., Gariépy, C., Ghaleb, B., Goy, J.L., Zazo, C., Barcelo, J.C., 1996. U-series measurements in Tyrrhenian deposits from mallorca - further evidence for two last-interglacial high sea levels in the Balearic Islands. Quat. Sci. Rev. 15 (1), 53–62.
Issel, A., 1914. Lembi fossiliferi quaternari e recenti nella Sardegna meridionale. Accad. Naz. Lincei (Fondazione Leone Caetani) 5, 759–770.
Jedoui, Y., Reyss, L., Kallel, N., Montacer, M., BenIsmayl, H., Davaud, E., 2003. U-series evidence for two high Last Interglacial sea levels in southeastern Tunisia. Quat. Sci. Rev. 22, 343–351.
Kellett, J., Balston, J., Western, M., 2014. Sea-level rise and planning: retrospect and prospect. Aust. Plan. 51 (3), 203–211.
Kopp, R.E., Simons, F.J., Mitrovica, J.X., Maloof, A.C., Oppenheimer, M., 2009. Probabilistic assessment of sea level during the last interglacial stage. Nature 462, 863–867.
Laborel, J., Laborel-Deguen, F., 1994. Biological indicators of relative sea-level variations and of co-seismic displacements in the Mediterranean region. J. Coast Res. 395–415.
Laborel, J., Laborel-Deguen, F., 2005. Sea-level indicators, biologic. In: Schwartz, M. (Ed.), Encyclopedia of Coastal Science. Wiley, New York, pp. 833–834.
Lambeck, K., Antonioli, F., Purcell, A., Silenzi, S., 2004. Sea-level change along the Italian coast for the past 10,000 yr. Quat. Sci. Rev. 23 (14–15), 1567–1598.
Lisiecki, L.E., Raymo, M.E., 2005. A Pliocene-Pleistocene stack of 57 globally distributed benthic δ18O records. Paleoceanography 20 (1).
Lončar, N., Faivre, S., Miklavič, B., Onac, B.P., Polyak, V.J., Asmerom, Y., 2024. Characterization of phreatic overgrowths on speleothems precipitated in the northern Adriatic during a sea-level stillstand at ca. 2.8 ka. Quat. Res. 118, 88–99.
Lucia, G., Polyak, V.J., Ginés, J., Fornós, J.J., Ginés, A., Asmerom, Y., Onac, B.P., 2021. Chronology of Middle pleistocene coastal karst evolution and Relative Sea-level changes in mallorca. J. Coast Res. 37 (2), 408–420.
Marra, F., Rolfo, F.M., Gaeta, M., Florindo, F., 2020. Anomalous last interglacial Tyrrhenian Sea levels and neanderthal settling at Guattari and Moscerini caves (central Italy). Sci. Rep. 10 (1), 11929 https://doi.org/10.1038/s41598-020-68604-z.
Martini, F., 2015. Cilento le Origini. Preistoria, arte e vita dei popoli cacciatori-raccoglitori. Museo e Istituto Fiorentino di Preistorioa, Firenze, p. 134.
Mauz, B., 1999. Late Pleistocene records of littoral processes at the Tyrrhenian Coast (Central Italy): depositional environments and luminescence chronology. Quat. Sci. Rev. 18, 1173–1184.
Monaco, L., Palladino, D.M., Albert, P.G., Arienzo, I., Conticelli, S., Di Vito, M., Fabbrizio, A., D'Antonio, M., Isaia, R., Manning, C.J., Nomade, S., Pereira, A., Petrosino, P., Sottili, G., Sulpizio, R., Zanchetta, G., Giaccio, B., 2022. Linking the Mediterranean MIS 5 tephra markers to Campi Flegrei (southern Italy) 109–92 ka explosive activity and refining the chronology of MIS 5c-d millennial-scale climate variability. Global Planet. Change 211, 103785.
Moseley, G.E., Smart, P.L., Richards, D.A., Hoffmann, D.L., 2013. Speleothem constraints on marine isotope stage (MIS) 5 relative sea levels, Yucatan Peninsula, Mexico. J. Quat. Sci. 28, 293–300.
Muhs, D.R., 2002. Evidence for the timing and duration of the last interglacial period from high-precision uranium- series ages of corals on tectonically stable coastlines. Quat. Res. 58, 36–40.
Muhs, D.R., Simmons, K.R., Meco, J., Porat, N., 2015. Uranium-series ages of fossil corals from Mallorca, Spain: the "Neotyrrhenian" high stand of the Mediterranean Sea revisited. Palaeogeogr. Palaeoclimatol. Palaeoecol. 438, 408–424.
O'Leary, M.J., Hearty, P.J., Thompson, W.G., Raymo, M.E., Mitrovica, J.X., Webster, J. M., 2013. Ice sheet collapse following a prolonged period of stable sea level during the last interglacial. Nat. Geosci. 6, 796–800.
Pasquetti, F., Bini, M., Giaccio, B., Vacchi, M., Zanchetta, G., 2021. Chronology of the Mediterranean sea-level highstand during the Last Interglacial: a critical review of the U/Th-dated deposits. J. Quat. Sci. 36, 1174–1189.
Peltier, W.R., Argus, D.F., Drummond, R., 2015. Space geodesy constrains ICE age terminal deglaciation, the global ICE-6G-C (VM5a) model. J. Geophys. Res. Solid Earth 120, 450–487.
Pieruccini, P., Forti, L., Mecozzi, B., Iannucci, A., Yu, T.-L., Shen, C.-C., Bona, F., Lembo, G., Mutillo, B., Sardella, R., Mazzini, I., 2022. Stratigraphic reassessment of Grotta Romanelli sheds light on Middle-Late Pleistocene palaeoenvironments and human settling in the Mediterranean. Sci. Rep. 2, 13530.

Pirazzoli, P.A., 2007. Sea level studies; geomorphological indicators. In: Elias, S.A. (Ed.), Encyclopedia of Quaternary Science. Elsevier, Oxford, pp. 2974–2983.
Pirazzoli, P.A., Laborel, J., Stiros, S.C., 1996. Earthquake clustering in the eastern mediterranean during historical times. J. Geophys. Res. Solid Earth 101, 6083–6097.
Polyak, V.J., Onac, B.P., Fornós, J.J., Hay, C., Asmerom, Y., Dorale, J.A., Ginés, J., Tuccimei, P., Ginés, A., 2018. A highly resolved record of relative sea level in the western Mediterranean Sea during the last interglacial period. Nat. Geosci. 11, 860–864.
Rohling, E.J., Hibbert, F.D., Grant, K.M., et al., 2019. Asynchronous Antarctic and Greenland ice-volume contributions to the last interglacial sea- level highstand. Nat. Commun. 10, 5040 [PubMed: 31695032].
Rolfo, M.F., Bini, M., Di Mario, F., Ferracci, A., Giaccio, B., Hsun-Ming, H., et al., 2023. Neanderthal bones collected by hyena at Grotta Guattari, central Italy, 66–65 ka: U/Th chronology and paleoenvironmental setting. Quat. Sci. Rev. 311, 108132.
Ronchitelli, A., Abbazzi, L., Accorsi, C.A., Bandini, Mazzanti M., Bernardi, M., Masini, F., Mercuri, A., Mezzabotta, C., Rook, L., 1998. Palethnological, Palynological and Paleontological data on the Grotta Grande of Scario e Salerno (Campania Southern Italy, 40°02'21"N/15°28'31"E). November 27. In: Proceedings of 1st International Congress on: Science and Technology for the Safeguard of Cultural Heritage in the Mediterranean Basin, pp. 1529–1535. Catania, Siracusa, Italy, Palermo. (Accessed 2 December 1995).
Ronchitelli, A., Boscato, P., Surdi, G., Masini, F., Petruso, D., Accorsi, C.A., Torri, P., 2011. The Grotta grande of Scario (Salerno, Italy): archaeology and environment during the last interglacial (MIS 5) of the mediterranean region. Quat. Int. 231, 95–109.
Rovere, A., Antonioli, F., Bianchi, C.N., 2015. Chapter 18. Fixed biological indicators. In: Shennan, A., Horton, B.P. (Eds.), Handbook of Sea-Level Research. Wiley & Sons Ltd, pp. 268–280.
Rovere, A., Raymo, M.E., Vacchi, M., Lorscheid, T., Stocchi, P., Gómez-Pujol, L., Harris, D.L., Casella, E., O'Leary, M.J., Hearty, P.J., 2016. The analysis of Last Interglacial (MIS 5e) relative sea-level indicators: Reconstructing sea-level in a warmer world. Earth Sci. Rev. 159, 404–427.
Rovere, A., Ryan, D.D., Vacchi, M., Dutton, A., Simms, A.R., Murray-Wallace, C.V., 2023. The world atlas of last interglacial shorelines (version 1.0. Earth Syst. Sci. Data 15, 1–23.
Sarti, L., 1996. Porto Infreschi (S. Giovanni a Pito, Salerno). Preistoria e Protostoria. Guide archeologiche. XIII Congr. Int. U.I.S.P.P., Forlì 1996, pp. 43–49.
Shen, C.-C., Wu, C.-C., Cheng, H., Lawrence Edwards, R.L., Hsieh, Y.-T.S., Chang, C.-C., Li, T.-Y., Lam, D.D., Kano, A., Hori, M., Spötl, C., 2012. High-precision and high-resolution carbonate ^{230}Th dating by MC-ICP-MS with SEM protocols. Geochem. Cosmochim. Acta 99, 71–86.
Shennan, I., Lambeck, K., Horton, B.P., Innes, J.B., Lloyd, J.M., McArthur, J.J., Purcell, T., Rutherford, M.M., 2000. Late Devensian and Holocene records of relative sea-level changes in northwest Scotland and their implications for glacio-hydroisostatic modelling. Quat. Sci. Rev. 19, 1103–1136.
Siddall, M., Rohling, E.J., Almogi-Labin, A., Hemleben, Ch, Meischner, D., Schmelzer, I., Smeed, D.A., 2003. Sea-level fluctuations during the last glacial cycle. Nature 423, 853–858.
Spagnolo, V., Crezzini, J., Falguères, C., Tombret, O., Garbe, L., Bahain, J.J., et al., 2024. Grotta Grande (southern Italy). Disentangling the Neandertal and carnivore interaction in a short-term palimpsest at the last glacial onset (~ 116-109 ka). Quat. Sci. Rev. 331, 108628.
Spratt, R.M., Lisiecki, L.E., 2016. A Late Pleistocene sea level stack. Clim. Past 12, 1079–1092.
Stewart, I.S., Morhange, C., 2009. Coastal geomorphology and sea-level change. The Physical Geography of the Mediterranean. Oxford University Press, Oxford, pp. 385–413.
Stirling, C.H., Esat, T.M., Lambeck, K., McCulloch, M.T., 1998. Timing and duration of the last interglacial; evidence for a restricted interval of widespread coral reef growth. Earth Planet Sci. Lett. 160, 745–762.
Stocchi, P., Vacchi, V., Lorscheid, T., de Boer, B., Simms, A.R., van de Wal, R.S.W., Vermeersen, B.L.A., Pappalardo, M., Rovere, A., 2018. MIS 5e relative sea-level changes in the Mediterranean Sea: Contribution of isostatic disequilibrium. Quat. Sci. Rev. 185 (122), 134.
Taviani, M., 2014. Unpersisting Persististrombus: a mediterranean story. Vieraea Folia Sci. Biol Canar 9–18.
Vacchi, M., Ermolli, E.R., Morhange, C., Ruello, M.R., Di Donato, V., Di Vito, M.A., Boetto, G., 2020. Millennial variability of rates of sea-level rise in the ancient harbour of Naples (Italy, western Mediterranean Sea). Quat. Res. 93, 284–298.
van de Plassche, O., 1986. Sea-level Research: A Manual for the Collection and Evaluationof Data. Geobooks, Norwich, p. 618.
Waelbroeck, L., Labeyrie, E., Duplessya, J.C., McManusc, J.F., Lambeck, K., Balbona, E., Labracherie, M., 2002. Sea-level and deep water temperature changes derived from benthic foraminifera isotopic records C. Quat. Sci. Rev. 21, 295–305.
Zanchetta, G., Bini, M., Isola, I., Pappalardo, M., Ribolini, A., Consoloni, I., Boretto, G., Fucks, E., Ragaini, L., Terrasi, F., 2014. Middle-to late-Holocene relative sea-level changes at Puerto Deseado (Patagonia, Argentina). Holocene 24, 307–317.
Zanchetta, G., Giaccio, B., Bini, M., Sarti, L., 2018. Tephrostratigraphy of Grotta del Cavallo, Southern Italy: insights on the chronology of Middle to Upper Palaeolithic transition in the Mediterranean. Quat. Sci. Rev. 182, 65–77.